frontiers in Ecology and Evolution

ORIGINAL RESEARCH
published: 22 December 2021
doi: 10.3389/fevo.2021.794728

Unique Habitat for Benthic Foraminifera in Subtidal Blue Holes on Carbonate Platforms

Shawna N. Little[1], Peter J. van Hengstum[2,3], Patricia A. Beddows[4†], Jeffrey P. Donnelly[5], Tyler S. Winkler[3,5] and Nancy A. Albury[6]*

[1] Department of Marine Biology, Texas A&M University, Galveston, TX, United States, [2] Department of Marine and Coastal Environmental Science, Texas A&M University, Galveston, TX, United States, [3] Department of Oceanography, Texas A&M University, College Station, TX, United States, [4] Department of Earth and Planetary Sciences, Northwestern University, Evanston, IL, United States, [5] Department of Geology and Geophysics, Woods Hole Oceanographic Institution, Woods Hole, MA, United States, [6] Coastal Cave Survey, West Branch, IA, United States

OPEN ACCESS

Edited by:
Sanda Iepure, Emil Racovita Institute of Speleology, Romanian Academy, Romania

Reviewed by:
Veronica Rossi, University of Bologna, Italy
Thomas Mark Cronin, United States Geological Survey, United States

***Correspondence:**
Shawna N. Little
Shawna88@tamu.edu

†ORCID:
Patricia A. Beddows
orcid.org/0000-0002-5482-5329

Specialty section:
This article was submitted to Population, Community, and Ecosystem Dynamics, a section of the journal Frontiers in Ecology and Evolution

Received: *14 October 2021*
Accepted: *30 November 2021*
Published: *22 December 2021*

Citation:
Little SN, van Hengstum PJ, Beddows PA, Donnelly JP, Winkler TS and Albury NA (2021) Unique Habitat for Benthic Foraminifera in Subtidal Blue Holes on Carbonate Platforms. Front. Ecol. Evol. 9:794728. doi: 10.3389/fevo.2021.794728

Dissolution of carbonate platforms, like The Bahamas, throughout Quaternary sea-level oscillations have created mature karst landscapes that can include sinkholes and off-shore blue holes. These karst features are flooded by saline oceanic waters and meteoric-influenced groundwaters, which creates unique groundwater environments and ecosystems. Little is known about the modern benthic meiofauna, like foraminifera, in these environments or how internal hydrographic characteristics of salinity, dissolved oxygen, or pH may influence benthic habitat viability. Here we compare the total benthic foraminiferal distributions in sediment-water interface samples collected from <2 m water depth on the carbonate tidal flats, and the two subtidal blue holes Freshwater River Blue Hole and Meredith's Blue Hole, on the leeward margin of Great Abaco Island, The Bahamas. All samples are dominated by miliolid foraminifera (i.e., *Quinqueloculina* and *Triloculina*), yet notable differences emerge in the secondary taxa between these two environments that allows identification of two assemblages: a Carbonate Tidal Flats Assemblage (CTFA) vs. a Blue Hole Assemblage (BHA). The CTFA includes abundant common shallow-water lagoon foraminifera (e.g., *Peneroplis*, *Rosalina*, *Rotorbis*), while the BHA has higher proportions of foraminifera that are known to tolerate stressful environmental conditions of brackish and dysoxic waters elsewhere (e.g., *Pseudoeponides*, *Cribroelphidium*, *Ammonia*). We also observe how the hydrographic differences between subtidal blue holes can promote different benthic habitats for foraminifera, and this is observed through differences in both agglutinated and hyaline fauna. The unique hydrographic conditions in subtidal blue holes make them great laboratories for assessing the response of benthic foraminiferal communities to extreme environmental conditions (e.g., low pH, dysoxia).

Keywords: The Bahamas, groundwater, benthic foraminifera, blue holes, karst landscapes, environmental stress

INTRODUCTION

Blue holes and sinkholes are common geomorphologic features on carbonate landscapes on low elevation eogenetic carbonate platforms like The Bahamas. They are commonly created by cave ceiling collapse, combined with flooding by deglacial sea-level rise, and concomitant vertical migration of local groundwater systems (Cole, 1910; Shinn et al., 1996; van Hengstum et al., 2011). Blue hole stratigraphic infill can preserve unique records of terrestrial ecology (Kjellmark, 1996; Steadman et al., 2007; Sullivan et al., 2020; Fall et al., 2021), hurricane activity (Lane et al., 2011; Wallace et al., 2019; Winkler et al., 2020; Wang et al., 2021), and physicochemical changes of the local groundwater in response to climate forcing (Teeter, 1995; van Hengstum et al., 2010; Peros et al., 2017). Regional hydroclimate change can also be preserved in the stratigraphy (Hodell et al., 2005; van Hengstum et al., 2016, 2018), which is caused by groundwater linkages to local precipitation-evaporation water balance (Cant and Weech, 1986; Whitaker and Smart, 1997). In terrestrial sinkholes, subfossil benthic meiofauna (e.g., ostracodes, benthic foraminifera, testate amoebe) assemblages and shell geochemistry are useful proxies of groundwater and environmental variability (Teeter, 1995; Zarikian et al., 2005; van Hengstum et al., 2008; Macario-González et al., 2021). In subtidal blue holes, however, it remains unclear if unique hydrographic conditions promote a unique foraminiferal habitat, or, if transported individuals from the adjacent marine environments including carbonate lagoons and mangroves are the primary control on resultant benthic foraminiferal total assemblages.

Benthic foraminifera are unicellular organisms that are highly sensitive to physicochemical changes in their surrounding environment, including pH, salinity, and dissolved oxygen. They are thus widely used proxies of marine environmental change. Foraminifera have been documented in horizontally expansive carbonate caves that are flooded by marine and brackish groundwater in the North Atlantic (Javaux and Scott, 2003; van Hengstum and Scott, 2011; van Hengstum and Bernhard, 2016; Little and van Hengstum, 2019) and Mediterranean regions (Romano et al., 2018; Bergamin et al., 2020). While unique benthic foraminiferal assemblages can be found in aquatic caves, individual benthic foraminifera are predictably governed by their ecological relationship with their physical environment in other coastal settings (Romano et al., 2020; Cresswell and van Hengstum, 2021). The water column in blue holes is often stratified: the surface water mass is a meteoric lens that is rainfall-influenced with lower density, and this is separated from dysoxic saline groundwater at depth by a mixing zone (Smart, 1984; Smart et al., 1988; Whitaker and Smart, 1997; Socki et al., 2002; Haas et al., 2018; Patin et al., 2020). van Hengstum et al. (2008) hypothesized that stratified hydrographic conditions in subtidal blue holes creates distinct benthic meiofaunal habitats, similar to terrestrial sinkholes, thus promoting distinct foraminiferal assemblages that can be differentiated from those observed in adjacent peritidal environments.

Here we compare recent benthic foraminiferal distributions on the shallow carbonate tidal flats (<2 m water depth) and two subtidal blue holes on the western margin of Great Abaco Island in the northern Bahamas (**Figure 1**). The main objective is to determine if an *in situ* assemblage of benthic foraminifera in subtidal blue holes can be detected, or if storm- and wave and/or current-induced transport of sediment and foraminiferal tests from adjacent shallow-water environments is a primary control on their foraminiferal assemblages. The focus of this paper is on recent foraminiferal distributions, so a detailed analysis of downcore foraminiferal assemblages and their environmental significance can follow elsewhere. Recent benthic foraminiferal distributions were investigated in surface-water interface samples collected from two subtidal blue holes on Abaco Island, and compared to (i) new sediment samples collected from the local carbonates tidal flats, and (ii) previously published results from other local marine environments (Rose and Lidz, 1977). To better understand hydrographic variability in the blue holes, water quality profiles of the water column were also collected though several seasons and compared to regional rainfall observed over a 30-month timespan.

STUDY SITE

The Bahamian Archipelago is a series of carbonate platforms and islands in the subtropical North Atlantic Ocean (**Figure 1**). Carbonate weathering and dissolution during the late Cenozoic has produced a karst landscape with abundant sinkholes, blue holes, and caves (Mylroie et al., 1995). The Little Bahama Bank is a dish-shaped carbonate platform, with the Grand Bahama and Great Abaco Islands separated by a shallow carbonate lagoon known as the Bight of Abaco (Neumann and Land, 1975; Pilskaln et al., 1989). During the last glacial maximum, the entire Little Bahama Bank was a subaerial landscape. Deglacial sea-level rise lifted the coastal aquifer (Rasmussen et al., 1990), and first internally flooded the Bight of Abaco ∼8800 years ago to create an inland water body. This event likely segmented the meteoric groundwater lens on the Little Bahama Bank (Gulley et al., 2016) and flooded previously dry sinkholes to create perennial aquatic habitats (van Hengstum et al., 2018, 2020). Mean Annual Precipitation (MAP) in the northern Bahamas is ∼1300 mm/year with a min/max range of 607 to 2334 mm/year from the Nassau rain gauge (data spans: 1855 to 2017 CE) on nearby New Providence Island, The Bahamas[1]. The average May-October rainy season rainfall during this time period is 990 mm/year (range: 442-1954 mm/year), and average November-April dry season rainfall is 316 mm/year (range: 88-766 mm/year). Tidal range on the Little Bahama Bank is ∼1 m, based on observations at the Pelican Harbor Tide Gauge on Abaco Island (Abaco Island[2]).

Carbonate tidal flats commonly occur on the leeward margin of Bahamian islands (Shinn et al., 1969; Maloof and Grotzinger, 2012), which includes the area known locally as "The Marls" (∼700 km^2) on the western margin of Great Abaco Island (**Figures 1**, **2**). The Marls is a restricted interior environment characterized by seawater circulation from the Bight of Abaco

[1]https://climexp.knmi.nl/start.cgi

[2]https://tidesandcurrents.noaa.gov/

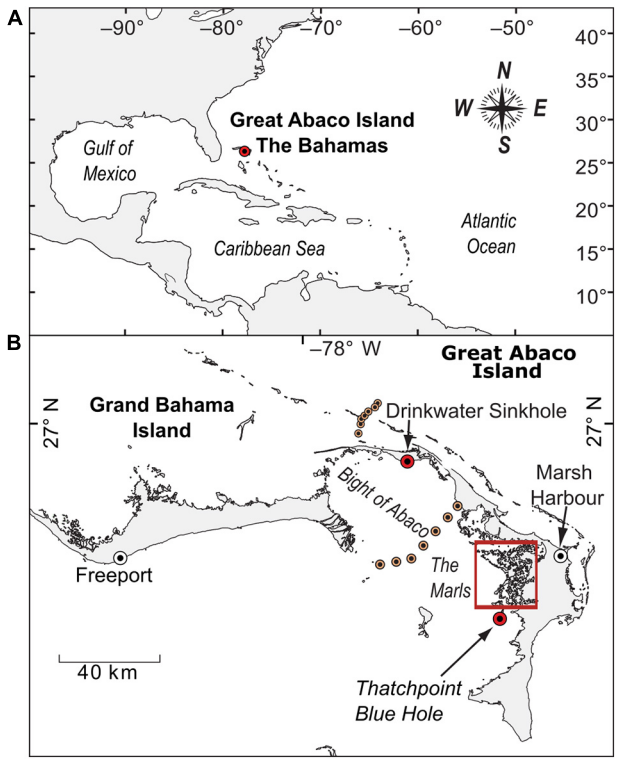

FIGURE 1 | (A) Map of The Bahamas with the location of Great Abaco Island in the tropical North Atlantic Ocean. **(B)** Map of Great Abaco Island indicating the positions of The Marls (red box) including Freshwater River Blue Hole (FRSH) and Meredith's Blue Hole (MERE), Drinkwater Sinkhole, the town of Marsh Harbour, and a nearby oceanic blue hole (Thatchpoint Blue Hole) that hosts tempestites (Winkler et al., 2020). Orange points are the locations from a transect of sediment-water interface samples studying modern benthic foraminiferal distributions in The Bahamas (Rose and Lidz, 1977).

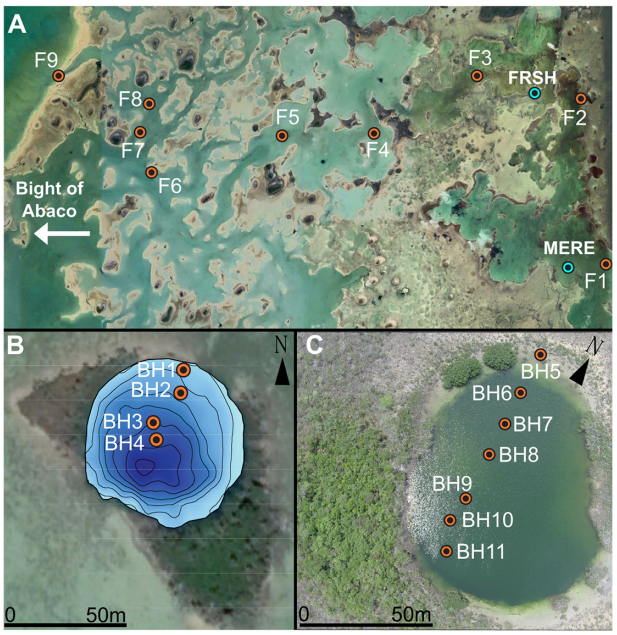

FIGURE 2 | Aerial imagery and sampling locations on **(A)** the carbonate tidal flats on the leeward side of Abaco Island. **(B)** Meredith's Blue Hole – MERE. **(C)** Freshwater River Blue Hole – FRSH. Blue circles indicate location of blue holes on the tidal flats. **(B,C)** Orange dots are locations of sediment-water interface grab samples.

driven by tides and winds, depth variability generated by the configuration of local mudbanks and unconsolidated sediment islands, and seasonal salinity variations from rainfall and evaporation. The area is habitat for abundant dwarf red mangrove trees (*Rhizophora mangle*, Rossi et al., 2020), which do not form mangrove peat deposits or peat islands, perhaps from local oligotrophic conditions (Koch and Snedaker, 1997) or salinity stress (Lin and Sternberg, 1992). Interestingly, The Marls does not have the archetypal carbonate tidal channels that are observed in northwestern Andros (Maloof and Grotzinger, 2012), which is perhaps related to differences in seawater volume exchanged during tidal cycles on the carbonate tidal flats of the Little Bahama Bank vs. Great Bahama Bank. Several subtidal blue holes are located in The Marls, such as our study sites of Freshwater River Blue Hole (**FRSH**, GPS: 26.426°, –77.175°) and Meredith's Blue Hole (**MERE**, GPS: 26.394°, –77.16°).

Surrounding Freshwater River Blue Hole (FRSH) is a >65 m radius of carbonate mudbank that is colonized by dwarf red mangrove, and the mudbank becomes just barely exposed during low tides (**Figures 3A-D**). The antecedent limestone locally outcrops within the mudbank and along the periphery of the blue hole. Prior to Hurricane Dorian (September 2019), a more mature mangrove stand was along the southwestern periphery of FRSH. A narrow channel on the eastern side connects FRSH to the adjacent subtidal waters and allows for the direct tidal exchange of seawater (**Figures 3B,D**). In the center of FRSH the sediment-water interface is ∼5 m below sea level (mbsl), and there is ∼360 cm of Holocene strata accumulated on top of a hardground, that is perhaps boulders from the original cave collapse. The stratigraphy in FRSH can be divided into a basal peat (8300 to 7600 years ago), lacustrine carbonate marl (7600 to 7000 years ago), then algal sapropel and lacustrine marl (7000 to 2300 years ago), and finally laminated marine carbonate mud (2300 years ago to present, van Hengstum et al., 2020). This stratigraphic sequence was generated by *in situ* environmental change in FRSH from concomitant Holocene relative groundwater and sea level-rise (van Hengstum et al., 2020). At the margins of the central talus pile, the bathymetry rapidly deepens and the blue hole is encircled by a cave that pinches-out at depths of 33 to 50 mbsl.

Meredith's Blue Hole (MERE) has sedimentary build-up on the north and south margins (∼400-550 m^2 in aerial extant), as well as two separate subtidal channels that allow direct seawater exchange into the blue hole from the surrounding carbonate tidal flats (**Figures 3E-H**). Mangrove peat deposits are found at the periphery of the subtidal channels at low tides, which indicates that MERE once had a more localized mangrove development. No similar mangrove peat deposits are observed at FRSH. Vegetation is densest on the southeastern edge of

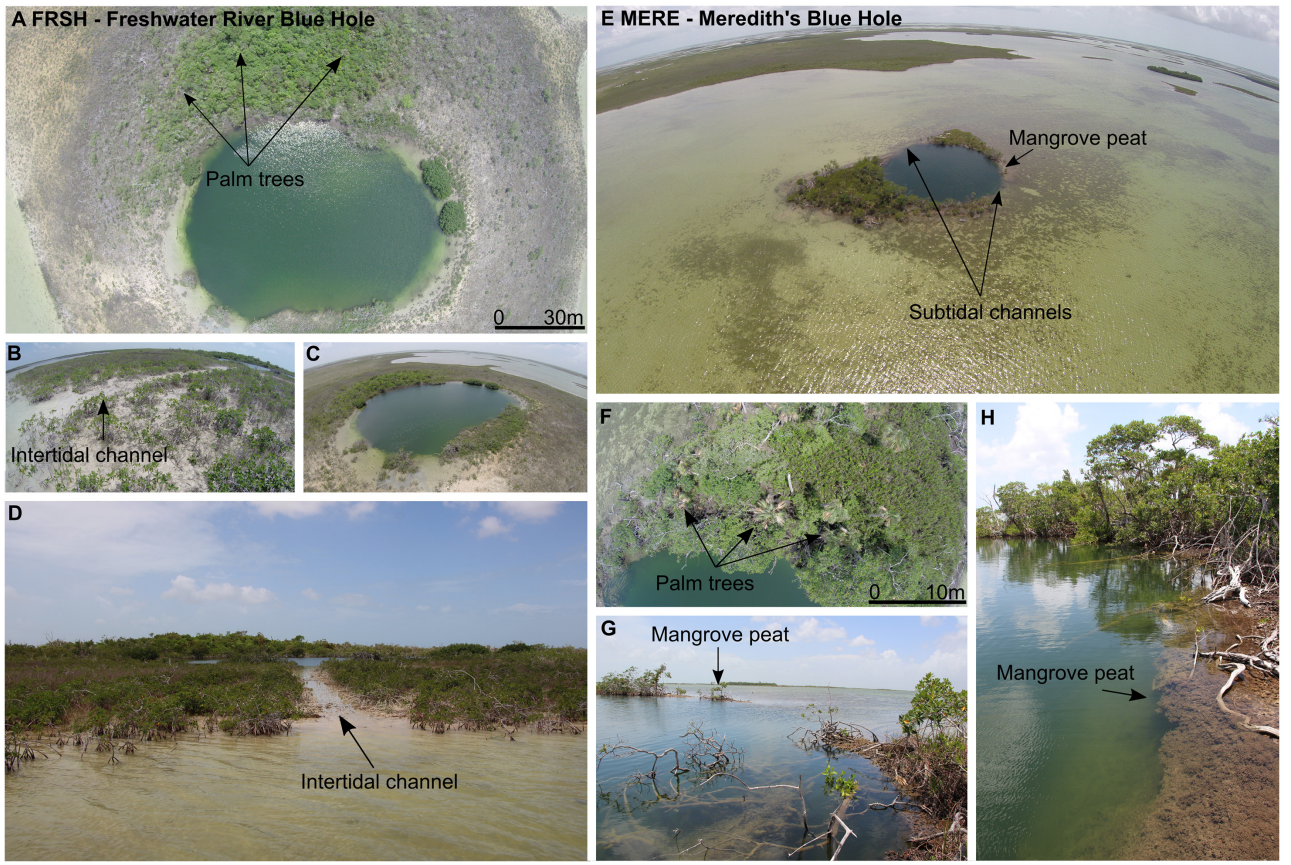

FIGURE 3 | (A–D) Photographs of Freshwater River Blue Hole (FRSH). **(A–C)** Aerial views highlight the carbonate mudbanks and surrounding vegetation around FRSH. Dwarf red mangroves inhabit the periphery of the blue hole, including the subtidal passageway on the eastern side of FRSH, ∼5 m wide **(D)**. **(E–H)** Aerial photographs of Meredith's Blue Hole (MERE). Aerial photographs of the blue hole surrounded by two, small landmasses on the northwestern and southeastern sides **(E)**, and overhead imagery of the dense vegetation situated on the southeastern edge **(F)**. **(G,H)** Similar to FRSH, the vegetation surrounding MERE is primarily composed of dwarf red mangroves, varying in height as both trees and shrubs. For scale, FRSH is ∼90 m in diameter, at its widest, while MERE is slightly smaller at ∼50 m in diameter.

MERE, with larger overhanging mangroves and a few palm trees (**Figures 3F,H**). Bathymetry in MERE slopes toward the SE to a maximum observed depth of 15 mbsl at the sediment water interface. It is currently unknown if human-sized caves are interconnected into MERE.

METHODS

Local Meteorological Conditions

Meteorological variables of rainfall, temperature, and barometric pressure were measured at two locations on Abaco Island: (i) Marsh Harbour (GPS: 26.532°, –77.060°), and (ii) Drinkwater Sinkhole (GPS: 26.686°, –77.624°). The stations used Cave Pearl Project data loggers set to 15 min sampling intervals (Beddows and Mallon, 2018) combined with Onset RGS tipping-bucket rain-gauge, and MS5803-05BA pressure and temperature sensors (sensor specifications in **Supplementary Table S1**). The Marsh Harbour station was positioned ∼4.5 m above the ground, with no aerial obstructions within 100 m, and it logged continuously from 29 January 2017 until 1 September 2019 (∼30 months). The second station was positioned ∼70 km north of FRSH and MERE to inform regional meteorological differences deemed particularly valuable since the long-term data from Nassau is from ∼150 km to the south. The instrument was positioned on a topographic high near an abandoned late 19th century two-story building from the Sisal Fiber Company located near Drinkwater Sinkhole (**Figure 1**; GPS: 26.686°, –77.624°) (Allen and Barbour, 1904). This station had no aerial obstructions within 500 m that could influence rainfall measurements, and it provides an overlapping dataset from 24 November 2018 to 13 July 2019 (∼8 months).

Blue Hole Water Column Structure

A YSI EXO1 multiparameter water quality sonde was used to measure vertical water column profiles in FRSH and MERE on 5 occasions over 4 years. As defined in multidecadal precipitation time series from the region (Jury et al., 2007), water profiling occurred during both the wet (May to October) and dry season (November to April). The YSI EXO1 measures

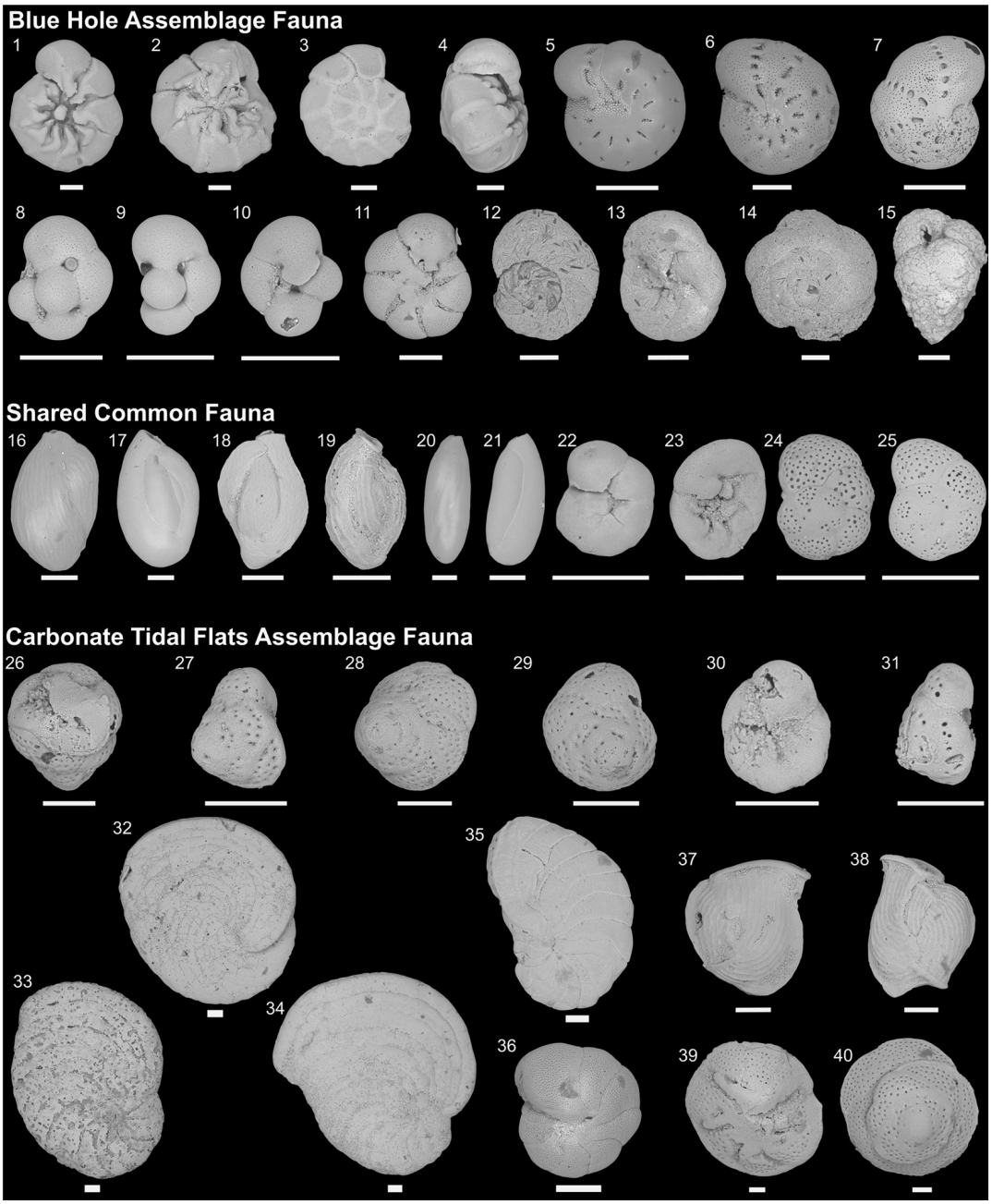

FIGURE 4 | New scanning electron microscope (SEM) images of characteristic taxa found in Freshwater River Blue Hole (FRSH), Meredith's Blue Hole (MERE), and The Marls (carbonate tidal flats). (1-4) Ammonia beccarii f. parkinsoniana (d'Orbigny, 1839a); (5,6) Cribroelphidium gunteri (Cole, 1931); (7) Cribroelphidium poeyanum (d'Orbigny, 1839a); (8-10) Pseudoeponides davescottensis (van Hengstum and Bernhard, 2016); (11) Pseudoeponides anderseni (Warren, 1957); (12) Entzia macrescens (Brady, 1870); (13,14) Tiphotrocha comprimata (Cushman and Brönnimann, 1948); (15) Globotextularia anceps (Brady, 1884); (16) Quinqueloculina laevigata (d'Orbigny, 1826); (17) Quinqueloculina seminulum (Linnaeus, 1758); (18) Quinqueloculina candeiana (d'Orbigny, 1839a); (19) Quinqueloculina tenagos (Parker, 1962); (20,21) Triloculina oblonga (Montagu, 1803); (22-25) Rosalina globularis (d'Orbigny, 1826); (26-29) Disconorbis sp.(?) (Sellier de Civrieux, 1977); (30-31) juvenile Disconorbis sp. (Sellier de Civrieux, 1977); (32) Archaias angulatus (Fichtel and Moll, 1798); (33-35) Laevipeneroplis proteus (d'Orbigny, 1839b); (36) Peneroplis pertusus (Forskål, 1775); (37,38) Articularia sagra (d'Orbigny, 1839a); (39,40) Rotorbis auberii (d'Orbigny, 1839a). All scale bars represent 100 μm.

depth (accuracy: ± 0.004 m), temperature (± 0.01°C), salinity (± 0.1 practical salinity units), pH (±0.1 pH units), and dissolved oxygen (±0.1 mg L^{-1}) at a sampling rate of 2 measurements per second. The sonde was typically calibrated within 48 h of deployment, and the pH probe was replaced annually to promote measurement integrity. Vertical density differences were calculated using the measured salinity and temperature parameters and input into Basin2 fluid flow

modeling calculations (Bethke et al., 2007). The individual vertical profiles were not corrected for the changing position of sea level from tides at the time of measurement, and therefore caution must be exercised when comparing changes in water column structure at intervals <1 m.

Benthic Foraminifera

Previous work has analyzed benthic foraminifera in the Bight of Abaco (Rose and Lidz, 1977; reviewed below), so we concentrated efforts on the carbonate tidal flats. Based on hydrodynamics in the tidal channels in south Andros (Wallace et al., 2019), our hypothesis was that storm-induced currents would be most elevated in the tidal channels, which would have the greatest potential for sediment erosion and transport from the carbonate tidal flats into the blue holes. In January 2018, samples ($n = 20$, upper 5 cm, ∼50 cm^3) were collected along a transect from the western periphery of the carbonate flats to the shoreline, including bottom sediment from FRSH and MERE (**Figure 2**), with all positions to ±3 m GPS horizontal uncertainty. Sediment at <1 m shallow water depths was collected by hand, with deeper sediment collected with an Eckman Grab Benthic Sampler. Water quality parameters were also concurrently collected at each sampling site on the carbonate tidal flats using the YSI EXO1 sonde. The water quality conditions measured during sampling represent a 'snapshot' within possible annual variability in an intertidal setting but do provide a framework for assessing the environmental setting where surficial benthic foraminiferal distributions were recovered.

Subsamples were first wet sieved over a 63-μm mesh sieve to concentrate benthic foraminiferal total assemblages. We respect the position of Murray (2000), which holds that total assemblages are limited in the ecological study of foraminifera, but total assemblages remain helpful in understanding sediment transport processes and generating time-averaged information that is most likely to be preserved in the stratigraphic record (Buzas, 1968; Scott and Medioli, 1980). Rose Bengal was not employed in this study to potentially identify living foraminifera at the time of collection. This is because benthic dysoxia can promote preservation of cytoplasm within the foraminiferal tests, and in turn may introduce bias from false-positive identification. The surface samples were wet-split (Scott and Hermelin, 1993; Charrieau et al., 2018), and individuals were wet-picked from resultant aliquots onto micropaleontological slides to preserve any agglutinated foraminifera (e.g., *Entzia*, *Trochammina*, and *Tiphotrocha*). A final census of >300 individuals per sample was sought to minimize standard error on the most dominant taxa (Patterson and Fishbein, 1989; Fatela and Taborda, 2002). Benthic foraminiferal taxonomy and designation primarily followed the World Register of Marine Species (WoRMS Editorial Board, 2021), and dominant taxa were imaged with a Hitatchi TM3000 TableTop scanning electron microscope (SEM) (**Figure 4**). When high taxonomic confidence existed, benthic foraminifera were identified to the species level in the raw database. However, in the final database certain species were grouped together at the genus level (e.g., juvenile *Quinqueloculina* and *Triloculina*, *Rosalina*, *Cribroelphidium*) as several porcelaneous taxa were commonly small and difficult to identify to the species level with confidence. This genus level grouping promotes a more robust identification of any differences in foraminiferal communities in the dataset. The final new database was produced for the 20 sediment samples includes 34 taxonomic units belonging to 23 genera.

Benthic foraminiferal raw counts were first converted to proportional abundances, and then square root transformed to emphasize community-level patterns (Legendre and Legendre, 1998). Biodiversity indices (rarefied species richness and Shannon-Weiner index) were calculated using the 'vegan' packages. Rarefied species richness was calculated due to the differences in final census counts (n) between samples (n range: 199 to 746 individuals), so the rarefaction was set to the lowest count of individuals present ($n = 199$ individuals) (Gotelli and Colwell, 2011; Colwell et al., 2012). Natural groupings of sample sites using the final benthic foraminifera database were determined with unconstrained Q-mode hierarchical cluster analysis using a Bray-Curtis dissimilarity distance and the unweighted pair-group method with arithmetic mean (UPGMA). Using a Similarity Profile (SIMPROF) test, the cluster analysis was subjected to 1000 permutations and a mean similarity profile generated with significant clusters ($p < 0.05$). The dendrogram from Q-mode cluster analysis was generated by the 'vegan' and 'clustsig' packages in R (R Core Team, 2021). A Similarity Percentage (SIMPER) analysis was used to further investigate the foraminiferal taxa primarily responsible for the dissimilarities between clusters, based on the Bray-Curtis dissimilarity values (Clarke, 1993; Warton et al., 2012). Differences in mean proportional abundances of dominant species between the resultant clusters were tested for significance ($p < 0.05$) using non-parametric means (Mann-Whitney test).

RESULTS

Benthic Foraminiferal Assemblages

All samples contained abundant benthic foraminifera, with miliolids forming the most dominant taxonomic group. This is an expected result for shallow-water carbonate settings (Carmen, 1927; Bock, 1971; Javaux and Scott, 2003). However, all samples contained a high number of notably smaller miliolid foraminifers belonging to the genera *Quinqueloculina* and *Triloculina*, as opposed to larger adult specimens that have a clear phenotype (e.g., *Triloculina linneana*, *Quinqueloculina auberiana*). The blue hole samples also had higher proportions of foraminifera with agglutinated tests vs. the carbonate tidal flats, especially samples from FRSH (**Figure 5**). Planktonic foraminifera were not observed in the samples from the restricted area of The Marls in Abaco, but they are also rare on the Great Bahama Bank (Todd and Low, 1971).

Q-mode cluster analysis separated the 20 samples into two groups at a Bray-Curtis dissimilarity of 0.41 (**Figure 6**), which we interpret to indicate two benthic foraminiferal assemblages: the Carbonate Tidal Flats Assemblage (CTFA) and the Blue Hole Assemblage (BHA) (**Figure 6**). However, the two samples collected near the intertidal shoreline (F1 and F2) were taxonomically more similar to samples collected

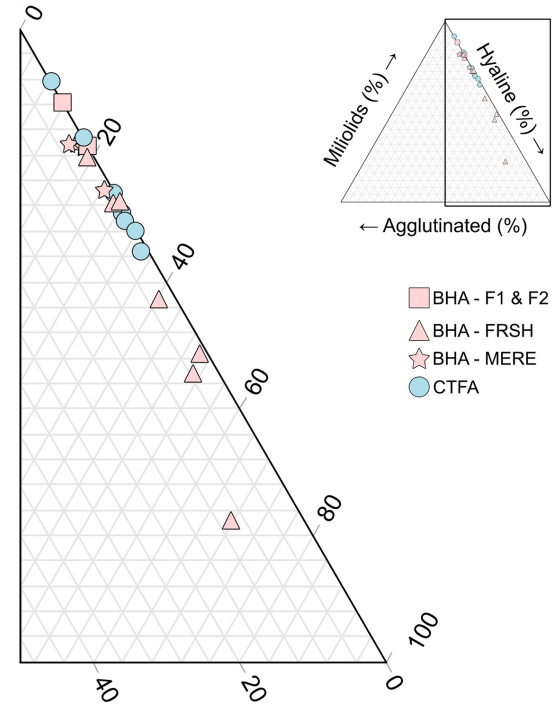

FIGURE 5 | Ternary plot of foraminiferal wall type in all samples ($n = 20$). Symbol color separates the CTFA (blue) vs. the BHA (pink). The BHA is further subdivided by origin (FRSH, MERE, vs. adjacent carbonate flats).

in the blue holes that form the BHA (discussed further below). Based on SIMPER analysis, ∼75% of the Bray-Curtis dissimilarity between the CTFA and BHA stems from differences in the relative abundance of *Triloculina*, *Quinqueloculina*, *Pseudoeponides*, *Rotorbis*, *Peneroplis*, and *Cribroelphidium* (**Table 1**). Comparing the proportional abundances of these taxa between assemblages yields statistically significant values: *Triloculina* (p-Value < 0.01), *Quinqueloculina* (p-Value < 0.01), *Peneroplis* (p-Value < 0.01), *Rotorbis* (p-Value < 0.01), *Pseudoeponides* (p-Value < 0.01). Nearly 50% of the differences between the assemblages can be attributed to the miliolid taxa *Triloculina* and *Quinqueloculina* alone.

The CTFA had a higher foraminiferal density (mean 18,353 individuals/cm^3, range: 2291 to 31,795 individuals/cm^3), a species diversity (H′) of 1.7, and a Species Richness (S_{rare}) of 13. The most abundant taxa belong to the miliolid genera *Quinqueloculina* (mean: 42%) and *Triloculina* (mean: 24%, **Table 1**). Other common taxa with mean proportions ≥ 5% in the CTFA include *Rotorbis* (7.4%), *Peneroplis* (6.8%), and *Rosalina* (5.0%), which are rare in the BHA (mean BHA: 0.91, 0.72, and 3.3% respectively) (**Figure 6** and **Table 1**). Less common fauna with mean proportions < 5% in the CTFA include *Cribroelphidium* spp. (2.2%), *Disconorbis* (4.4%), and *Buliminella* (1.1%), with the remainder of the assemblage composed of rare taxa (<1% proportional abundance). The exclusion of the shoreline proximal samples F1 and F2 primarily stems from the lack of taxa which characterize the CTFA, namely, *Rotorbis*, *Peneroplis*, and *Rosalina* at mean proportions of 0%, 0.9%, and 0.4% respectively.

In contrast, the BHA had a lower benthic foraminiferal density (mean: 2925 individuals/cm^3, range: 39 to 28,979 individuals/cm^3) relative to the CTFA. Furthermore, if the samples from the shoreline (F1 and F2) are excluded, benthic foraminiferal density in the blue holes is at least an order of magnitude lower than in the CTFA (only FRSH and MERE, mean: 502 individuals cm^{-3}). The BHA had a similar diversity (H′ = 1.6) and species richness (S_{rare} = 13) as the CTFA. The mean proportions of miliolids like *Triloculina* (39%) and *Quinqueloculina* (29%) remained dominant, albeit at slightly different proportions than the CTFA. However, *Cribroelphidium* (mean: 8.0%), *Pseudoeponides* (mean: 7.5%), *Ammonia* (mean: 3.5%), and *Rosalina* (mean: 3.3%) were more common in the BHA. Agglutinated foraminifera like *Entzia*, *Tiphotrocha*, and *Trochammina* were not common in the BHA (mean: 1.9%), but their presence is significant as agglutinated taxa were rare in the CTFA with only *Globotextularia* (mean: 0.4%; **Figure 5**). Similarly, *Fissurina* is uncommon in the BHA (mean: 2.1%), but it is almost entirely absent in the CTFA (mean: 0.2%).

Abaco Rainfall, Temperature, and Atmospheric Pressure (January 2017 to September 2019 CE)

In Marsh Harbour, 30 months of meteorological measurements document two annual cycles (**Figure 7**). We define the hydrological year beginning at the start of recharge season as **Year 1** from 1 May 2017 to 30 April 2018 and **Year 2** from 1 May 2018 to 30 April 2019, following divisions that emerge in long-term multi-decadal meteorological time series (Jury et al., 2007).

Mean Annual Precipitation (MAP) in Year 1 and Year 2 was 1091 mm/year and 809 mm/year, respectively (**Table 2**). More rainfall was recorded in Year 1 during both the wet (608 vs. 505 mm) and dry seasons (483 vs. 304 mm). The 2017/18 dry season data had two large > 40 mm/day rainfall events occurring on 8 December 2017 and 11 January 2018. Comparatively, the dry season of Year 2 had one on 3 November 2018, which is arguably the tail-end of the wet season. In the Year 1 2017 wet season, three major rainfall events with > 40 mm/day contributed ∼25% of the wet season rainfall for that year, on 15 August, and a two-day event on 4-5 October. The remainder of the wet season is marked by frequent, small rainfall events of > 5 mm/day. By comparison, the 2018 wet season only experienced 1 major rainfall event (> 40 mm/day), and similar frequent lighter precipitation events. In comparison to long-term rainfall from 1855 to 2017 CE observed at the Nassau rain gauge that is in a similar meteorological zone (Jury et al., 2007), the observed rainfall values from Marsh Harbour (Abaco) are within expected values, but at the lower end of the potential range. Average air temperatures in Marsh Harbour were similar during the wet season (Year 1: 27.8°C, Year 2: 27.5°C) and dry season (Year 1: 22.1°C, Year 2: 23.0°C) during both years.

The weather data from the Drinkwater Sinkhole station has an ∼8 month overlap with the Marsh Harbour record from 24 November 2018 through 14 July 2019, allowing for a near

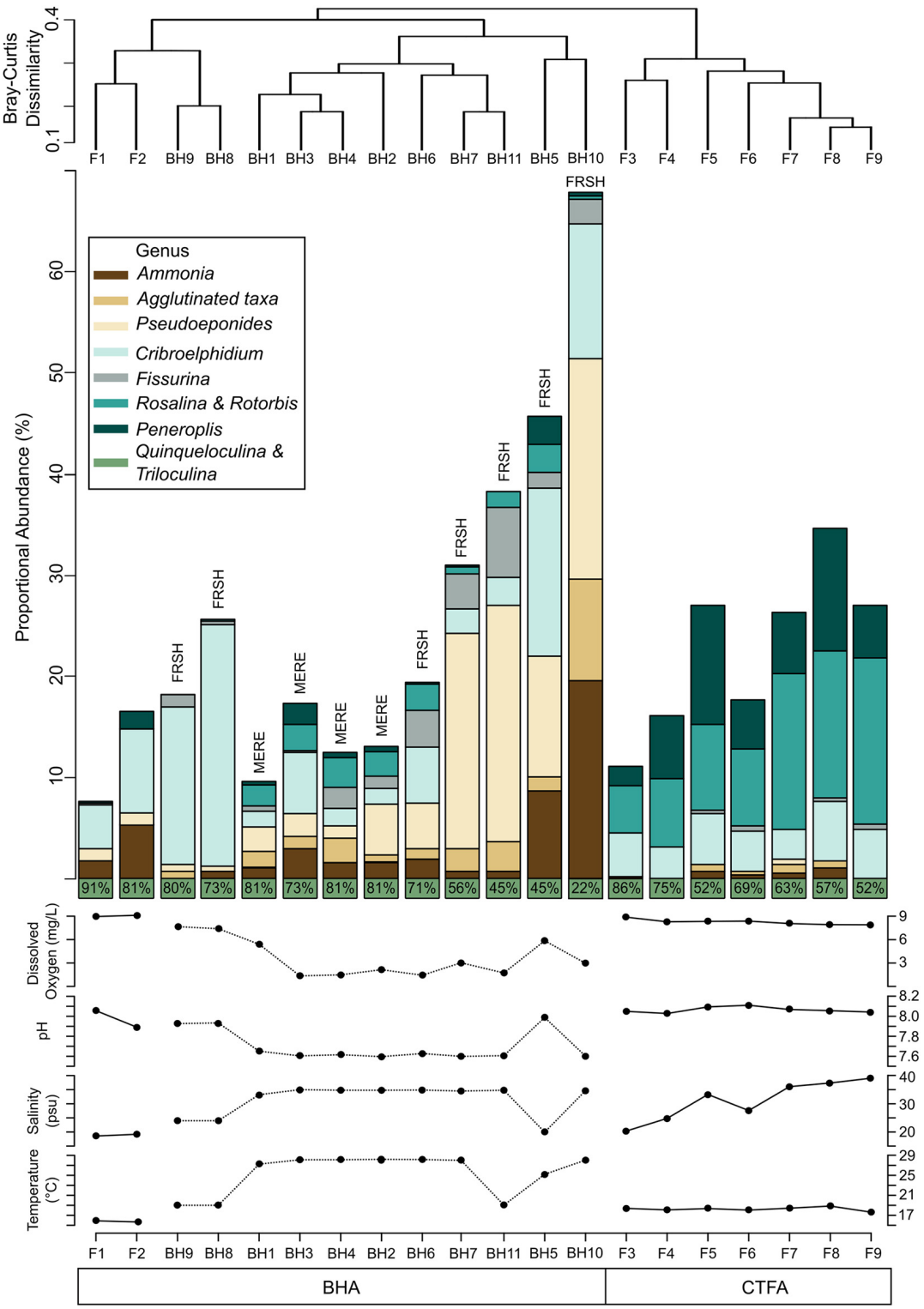

FIGURE 6 | (Top) Dendrogram produced from Q-mode cluster analysis groups surface samples into two assemblages: the Blue Hole Assemblage (BHA; green) and the Carbonate Tidal Flats Assemblage (CTFA; blue). (Middle) Stacked bar plots are the proportional abundance of the taxa present at >5% in at least one sample. To emphasize the subtle shifts in faunal abundance of less dominant taxa, Quinqueloculina and Triloculina are displayed separated at the base of the bar plot with their combined proportional abundance. Samples are organized by dendrogram grouping and proximity to the shoreline. (Bottom) Physicochemical parameters measured at the time of sample collection. Parameters were recorded at each site along the carbonate tidal flats while measurements for the blue hole samples are approximated from the water column profiles during sediment-water interface sample collection.

TABLE 1 | Mean proportional abundance of species significant to both the Blue Hole Assemblage (BHA) and Carbonate Tidal Flats Assemblage (CTFA) with Similarity Percentage (SIMPER) analysis output including *p*-Values testing significant comparisons between assemblages.

Taxa	BHA mean proportion	CTFA mean proportion	Average dissimilarity	% contribution	*p*-Value
Triloculina	38.6	24.0	9.55	23.3	<0.05*
Quinqueloculina	28.9	42.0	8.96	21.9	<0.05*
Pseudoeponides	7.51	0.06	3.73	9.11	<0.01*
Rotorbis	0.92	7.40	3.26	7.97	<0.01*
Peneroplis	0.72	6.81	3.10	7.57	<0.01*
Cribroelphidium	7.99	4.30	2.75	6.71	0.12
Ammonia	3.49	0.33	1.62	3.95	<0.01*
Rosalina	3.30	5.00	1.49	3.64	0.15
			Overall dissimilarity: 41.2		

The asterisk (*) indicates statistically significant p-Values.

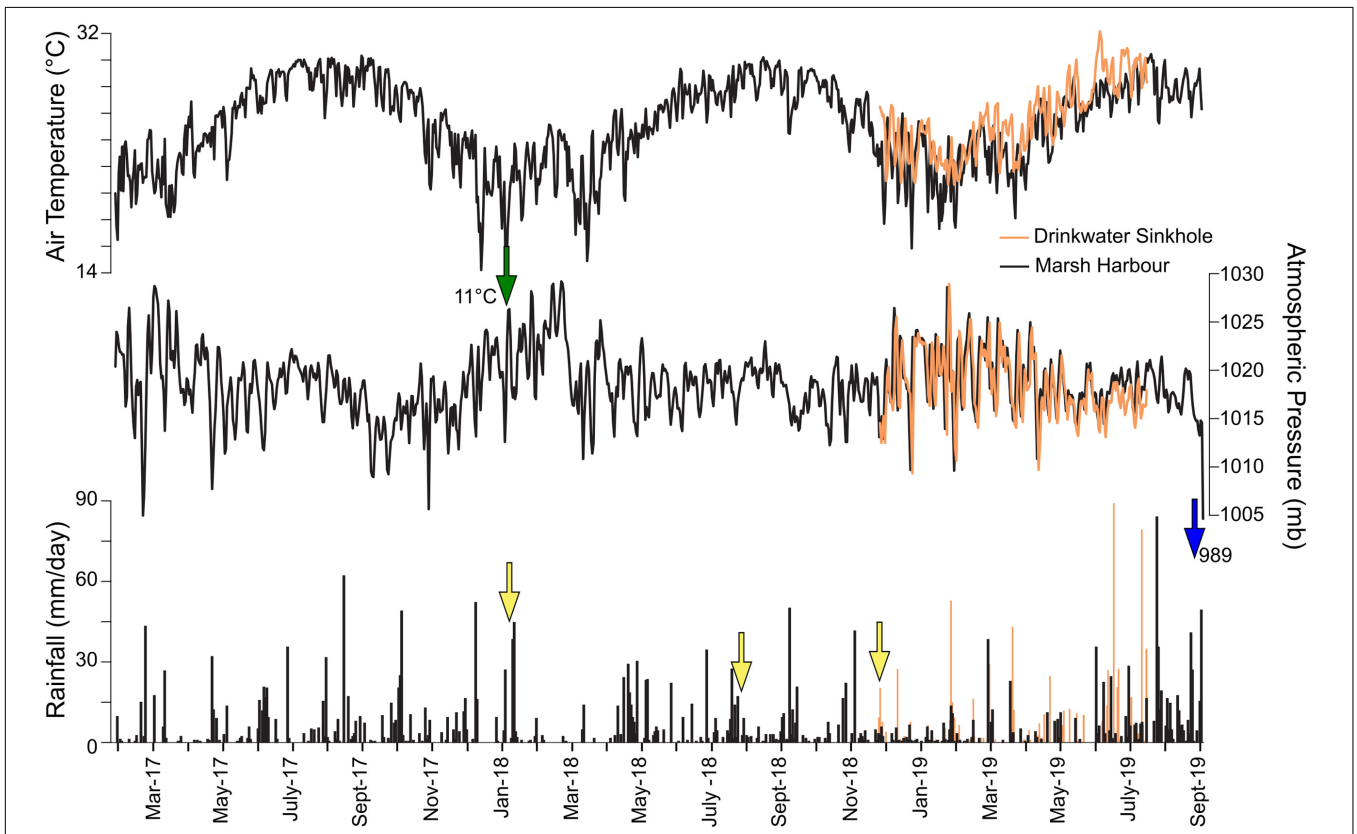

FIGURE 7 | Air temperature (°C), atmospheric pressure (mb), and daily rainfall (mm/day) from two rain gauge stations on Abaco Island, The Bahamas. The Marsh Harbour Kenyon Research Center (black) deployed from January 2017 through July 2019 while the Drinkwater Sinkhole (orange) gauge recorded from November 2018 through July 2019. The green arrow indicates a drop in air-temperature related to the storm event on 8 January 2018 that caused meteorically influenced ground water to discharge out of Meredith's Blue Hole. The yellow arrows indicate time points where water column profiles were collected. The blue arrow is final measurement recorded during Hurricane Dorian (Category 5 event on the Saffir Simpson Scale, 1 September 2019).

complete comparison of the Year 2 dry season (**Figure 7**). At Drinkwater Sinkhole, monthly rainfall totals were lowest in winter (December 2018: 37 mm) and highest during boreal summer (June 2019: 216 mm) (**Table 2**). Geographic variability in mean rainfall totals was limited between these two sites, with Drinkwater Sinkhole receiving comparable rainfall of 391 mm to the 401 mm in Marsh Harbour, but with a greater amount of winter rainfall at 357 mm to the 241 mm in Marsh Harbour. Daily rainfall distribution varies between locales, as seen in four instances of major > 40 mm/day rainfall events at Drinkwater Sinkhole on 25 January 2019 (53 mm), 19 March 2019 (43 mm), 14 June 2019 (89 mm), and 8 July 2019 (79 mm), of which none of these were recorded at the more southerly Marsh Harbour station.

Similar atmospheric pressure and air temperature was recorded at the two locations. The average air temperature

TABLE 2 | Meteorological statistics from the rain gauge deployed at Marsh Harbour, at the Kenyon Research Centre, Abaco Island, Bahamas between May 2017 and April 2019.

		Year 1 2017 – 2018		Year 2 2018 – 2019	
		WET May – October	**DRY November – April**	**WET May – October**	**DRY November – April**
Rainfall (mm)	Annual total (mm)	1092		810	
	Range	0 – 62.0	0 – 52.2	0 – 50.0	0 – 41.4
	SD (σ)	8.51	7.60	1.55	4.94
	Seasonal totals (mm)	608	483	505	304
Temperature (°C)	Range	13.2 – 36.2	7.77 – 32.1	16.6 – 35.3	10.5 – 33.7
	SD (σ)	1.88	2.54	2.06	2.32
Pressure (mbar)	Range	1001.7 – 1023.3	1006.1 – 1030.6	1010.2 – 1024.6	1005.5 – 1030.9
	SD (σ)	3.02	3.95	2.19	3.32

SD, standard deviation.

in Marsh Harbour was 27.5°C in the wet season and cooler at 22.9°C in the dry season, with similar values observed at Drinkwater Sinkhole (wet: 26.6°C; dry: 21.6°C) (**Table 2**). Barometric pressure at Marsh Harbour averaged 1018 mbar for the wet season and 1019 mbar for the dry season, with similar values recorded at the northern station (Drinkwater Sinkhole) at 1017 and 1019 mbar for the wet and dry season, respectively. The final abrupt decrease in air pressure was from passage of Category 5 Hurricane Dorian on 1 September 2019, with barometric pressure dropping to 989.3 mbar at Marsh Harbour (**Figure 7**, blue arrow).

Blue Hole Water Column Structure

To evaluate the water column structure in the blue hole, we follow Beddows et al. (2007) and delimit isohaline and isothermal waters to differentiate the lower saline groundwater mass (**SGW**), a transitional mixing zone (**MZ**), and the surficial meteoric lens (**ML**) that is directly affected by rainfall and evaporation.

The water column in MERE is generally stratified, with a defined ML from 0 to 2 mbsl, a transitional MZ from 2 to 6 mbsl, and SGW that begins > 6 mbsl (**Figure 8B**). Salinity in the ML is mean 20.7 ± 2.7 psu, which is up to 20 psu lower than the edge of the surrounding carbonate tidal flats (**Figure 3**, F9), and ∼3 to 9 psu lower than the upper water column in FRSH. The ML at MERE is generally the warmest watermass (mean: 27.8 ± 1.9°C), although temperatures vary seasonally (**Table 3**). Wave-based mixing, atmospheric gas exchange, and tidal exchange of seawater into the blue hole cause the ML to be well oxygenated (mean: 5.3 ± 0.6 mg/L) with normal surface ocean pH values (mean: 8.1 ± 0.2). The MZ can be identified as a pycnocline that has lower salinities (mean: 27.9 ± 6.2 psu) and lower dissolved oxygen concentrations (mean: 2.6 ± 2.0 mg/L) than the ML, with depth varying seasonally from 2 to 6 mbsl. At deeper depths, the SGW is the coldest (mean: 25.3 ± 0.2°C) and most saline (mean: 36.0 ± 1.9 psu) watermass observed in MERE, with a neutral pH (mean: 7.1 ± 0.02) and the water is nearly anoxic (mean: 0.2 ± 0.1 mg/L). The sediment-water interface in MERE is at 13 mbsl, with the benthos most commonly flooded by the anoxic SGW throughout the calendar year.

Hydrographic conditions in FRSH are completely different from MERE, despite the blue holes being only ∼3.5 km apart. The MZ and ML in FRSH are highly variable over time, with less defined boundaries, and more sensitive to changing environmental conditions. For example, a clearly defined ML was observed in the dry season on 29 May 2014 down to 5 mbsl with mean salinity of 29.0 psu, and a thinner but still well-defined, ML on 6 January 2018 (0 to 3.5 mbsl, mean salinity: 23.6 psu). Wet season observations show a poorly defined ML on 28 July 2018 and also on 25 November 2018 two months from the end of the wet season. Not only is the wet season ML less well defined, but the ML was completely absent on 1 July 2016, with the entire water column being isohaline (mean: 32.9 ± 0.89 psu). When water column profiles from FRSH are considered together, there is an upper water column from 0 to 6 mbsl with highly variable temperature ranging from 25.7 to 38.9°C, salinity ranging from mid-brackish to full marine (18.2 to 36.2 psu), pH from acidic to alkaline ranging 6.7 to 8.1, and dissolved oxygen from anoxic to oxic (0.3 to 6.2 mg/L). With the ML reaching 6 mbsl, these are the hydrographic conditions that characterize the top of the talus pile at ∼5.5 mbsl in the middle of FRSH. Surrounding the central talus pile below 6 mbsl, and into the overhang or cave area that surrounds the blue hole, more stable hydrographic conditions occur in the SGW. The SGW has an average salinity of (34.9 ± 1.5 psu), a temperature of 25.0 ± 0.4°C, and a pH of 7.0 ± 0.1, and is most likely anoxic (mean: 0.2 mg/L ± 0.1). The standard deviation of the hydrochemical factors is small and relatively invariant, especially compared to the ML (**Table 3**).

The water column structure on 6 January 2018 provides a case study on the contrasting hydrological conditions between the two blue holes, so the 6 January 2018 data was not averaged with the other vertical profiles in the summary statistics reported above (unless stated otherwise). On 3 January 2018, the United States National Weather Service observed a low-pressure system originating in the northern Bahamas as it developed into a north-northeast tracking winter storm that impacted the eastern United States with heavy precipitation (i.e., snow and rainfall) and low atmospheric temperatures. The effects of this winter storm on Abaco were observed on 6 January 2018, causing local extreme low air temperatures of 11°C, which is ∼ 10°C lower than winter mean temperatures of 22.1°C (**Table 2**), and 31 mm of rainfall fell over 2 days. In FRSH, a ML developed from 0 to 3.5 mbsl with mean salinity and temperature of 23.6 psu and 18.6°C,

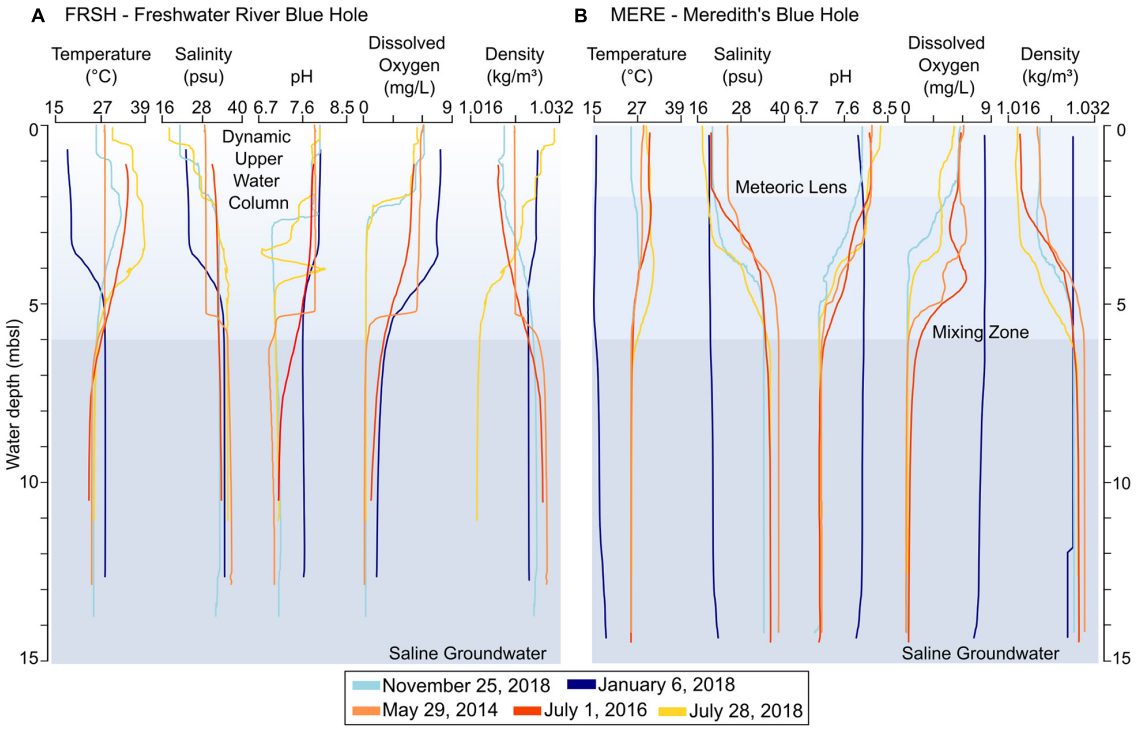

FIGURE 8 | Water column hydrographic profiles collected from **(A)** Freshwater River Blue Hole (FRSH) and **(B)** Meredith's Blue Hole (MERE) across multiple years (2014-2018) during the dry seasons (blues) and wet seasons (orange-yellow). Decent rate of instrument was ~1 cm/s during profiling, with a sampling frequency of 1 Hz. Plotted profiles are generated using a 10-point moving average of the recorded vertical changes. ML: Meteoric lens, MZ: mixing zone, and SGW: saline groundwater. The upper water column in FRSH is variable and cannot be designated into a distinct ML and MZ.

TABLE 3 | Statistics of the physicochemical parameters measured in Freshwater River Blue Hole (FRSH) and Meredith's Blue Hole (MERE).

	Meredith's Blue Hole - MERE			Freshwater River Blue Hole - FRSH	
	ML meteoric lens	**MZ mixing zone**	**SGW saline groundwater**	**Upper water column**	**SGW saline groundwater**
Temperature (°C)	27.8 ± 1.9	27.7 ± 1.7	25.3 ± 0.2	29.9 ± 3.7	25.0 ± 0.4
Salinity (psu)	20.7 ± 2.7	27.9 ± 6.2	36.0 ± 1.9	29.6 ± 3.8	34.9 ± 1.5
pH	8.1 ± 0.2	7.6 ± 0.4	7.1 ± 0.0	7.6 ± 0.4	7.1 ± 0.1
Dissolved oxygen (mg/L)	5.32 ± 0.62	2.62 ± 2.0	0.23 ± 0.1	3.79 ± 2.5	0.21 ± 0.1
Density (g/cm^3)	1.02 ± 1.9^{-03}	1.03 ± 3.5^{-03}	1.03 ± 8.9^{-04}	1.02 ± 2.4^{-03}	1.03 ± 3.9^{-03}

In MERE, the water column can be distinguished as three distinct water masses, each with different mean values while FRSH can only be separated into the bottom saline groundwater layer and an upper water column (<6 m).

respectively. The ML had high dissolved oxygen concentrations of 7.7 mg/L and a pH of 7.9 (**Figure 8A**). Below the ML was a well-defined MZ from 3 to 5.5 to 6 mbsl, with higher salinity (mean: 31.4 psu) and temperature (25.8°C), and lower dissolved oxygen (5.1 mg/L) and pH (7.7). These conditions elevated the dissolved oxygenation concentrations at the sediment-water interface at the top of the talus pile in the center of FRSH to a mean value of 1.6 mg/L (min: 1.3 mg/L) and increased bottom water temperature to 28.2°C. Salinity was normal marine conditions (~35 psu) with pH exceeding 7.5. In MERE, the 6 January 2018 water column is notably homogenous (**Figure 8B**): low temperature (15 to 18.6°C), low salinity (19 and 22 psu), normal surface ocean pH values (range: 7.8 to 8.0) and dissolved oxygen concentrations (range: 6.7 to 8.4 mg/L). This differs markedly from all other profiles that show a stratified water column in MERE.

DISCUSSION

Marine Benthic Foraminifera of The Marls

Miliolid foraminifera (*Quinqueloculina*, *Triloculina*, *Archaias*, and *Peneroplis*) dominating the shallow marine settings on Great Abaco Island is not surprising because miliolids are widespread on shallow carbonate platforms in the tropics and subtropics (Culver and Buzas, 1982; Li and Jones, 1997; Javaux and Scott, 2003). However, the detailed changes in foraminiferal

assemblages between the Bight of Abaco (carbonate lagoon) and The Marls (carbonate tidal flats) follow regional taxonomic shifts between more open ocean, to restricted, and finally shoreline proximal sub-environments on carbonate platforms (Todd and Low, 1971). On nearby Great Bahama Bank, for example, subtidal lagoons are dominated by *Archaias angulatus* (Fichtel and Moll) and *Peneroplis proteus* d'Orbigny, with more restricted and nearshore areas dominated by *Discorbis aguayoi*, *Elphidium morenoi*, *Helenina anderseni* and *Parrina bradyi* (Millet) (Todd and Low, 1971). In the carbonate embayment of Florida Bay (∼1550 km^2), the miliolid genera such as *Triloculina linneiana*, *Quinqueloculina lamarckiana* and *Archaias angulatus* are most dominant near the open ocean. Moving proximal to the shoreline, foraminiferal assemblages in Florida Bay are dominated by *Elphidium discoidale* and *Ammonia beccarii* (Bock, 1971; Lidz and Rose, 1989; Brewster-Wingard and Ishman, 1999; Cheng et al., 2012), likely in response to high organic carbon content and lower salinity (Verlaak and Collins, 2021). In the Bight of Abaco, Rose and Lidz (1977) similarly observed that *Archaias angulatus* formed 80% of the benthic foraminiferal assemblage in the subtidal lagoon, but there has not been an analysis of foraminifera on the carbonate tidal flats.

Our new results indicate that the genera *Archaias* and *Peneroplis* do not dominate the Carbonate Tidal Flats Assemblage (CTFA, **Figure 6**) of The Marls, in terms of abundance of the total assemblage (**Figure 6**), and that the abundance of common euryhaline taxa like *Cribroelphidium, Pseudoeponides*, and *Ammonia* increase with proximity to the shoreline (**Figures 2**, **6**, samples F1 and F2). Less abundant genera in the CTFA include *Rosalina* and *Rotorbis*, which are also common in coastal carbonate settings in The Bahamas and elsewhere (Rose and Lidz, 1977; Lidz and Rose, 1989; Fischel et al., 2018). These taxonomic transitions in Abaco are consistent with previous ideas that seawater circulation rates, water depth from subtidal through supratidal zones, and salinity variations from local water balance, often controlled by precipitation:evaporation ratios, are important regulators of benthic foraminiferal assemblages on shallow carbonate platforms in humid climates. On the windward shore of Abaco, which does not have carbonate tidal flats, coarse sediment on some beaches can be dominated by tests of *Archaias angulatus* that have been transported landward from the Sea of Abaco (van Hengstum et al., 2016). These results indicate that foraminiferal biogeographical distributions, the presence of subaerial landforms on the leeward sides of the island, and common particle transport processes can promote different foraminiferal total assemblages on the windward vs. leeward sides of carbonate islands.

Benthic Foraminifera in Unique Blue Hole Environments

In the two blue holes examined, the density of benthic foraminifera was an order of magnitude lower than in the adjacent subtidal habitats (CTFA). The foraminiferal assemblages were also dominated by miliolid foraminifera (**Figures 4**, **5**), but the larger *Archaias* and *Peneroplis* genera that are common in the Bight of Abaco and carbonate tidal flats were rarely observed in the blue holes. Furthermore, the miliolids were notably small in size, hampering species-level taxonomic designation based on morphology alone. Based on the observed hydrographic conditions of lowered pH and near anoxia (**Figure 8**), the benthic conditions in MERE and FRSH are generally incompatible with the ecology of miliolid and other foraminifera. For example, in normal seawater close to benthic CO_2 seeps in Papua New Guinea, benthic foraminifera are absent when pH was less than 7.8-7.9, with the genera *Elphidium* having slightly better adaptation to lower pH (Uthicke et al., 2013). In experimental cultures of Saraswat et al. (2011), the common shallow water taxon *Rosalina globularis* experienced test calcification and reproductive deficiencies when cultured in brackish water with lowered pH (10 psu and 7.2 pH, and 15 psu with 7.5 pH), and foraminiferal tests eventually dissolved (in 24 and 43 days, respectively). In the deep-sea, larger miliolid taxa are most prevalent in oxic environments (>2 mg/L), while smaller individuals may persist in suboxic conditions (0.3-1.5 mg/L), as most miliolids are intolerant of anoxia (Kaiho, 1994, 1999; Gooday et al., 2000).

At least two possibilities emerge to explain the abundance of smaller miliolids in FRSH and MERE. First, the smaller miliolids may be transported from the adjacent subtidal settings into the blue hole, either as empty tests or living individuals. The Little Bahama Bank is frequently hit by hurricanes (Winkler et al., 2020) and storms, which preferentially export finer carbonate sediment off the banktop and concentrate coarser particles in the Bight of Abaco (Neumann and Land, 1975). On the Island of Nevis, Wilson (2006) hypothesized that storm-winnowing of smaller benthic foraminifera contributed to the high percentage (>45%) of *Archaias angulatus* in lagoonal assemblages. Given that benthic foraminifera are well-established sediment transport indicators (Hawkes et al., 2007; Pilarczyk et al., 2011) and that *Archaias* and *Peneroplis* are rarely observed in the BHA (**Figure 6**, max. 13 individuals in BH5) and not common in the CTFA by proportion of total assemblage, it is hard to conclude that storms are causing wholesale transport of coarse sediment from the lagoon environment (Bight of Abaco) into the carbonate tidal flats (The Marls). More specifically, while intense hurricanes (e.g., Floyd in 1999 and Jeanne in 2004) developed coarse-grained tempestites in Thatchpoint Blue Hole in the Bight of Abaco (Winkler et al., 2020), these storms did not deposit similar tempestites in Freshwater River Blue Hole (van Hengstum et al., 2020). From a sediment transport perspective, the lack of coarse-grained tempestites dominated by larger miliolids (e.g., *Archaias*, *Peneroplis*) in the stratigraphy of FRSH indicates that more complex hydrodynamics and sediment processes are occurring in the carbonate tidal flat depositional environment (e.g., Wallace et al., 2019). While the microfossil results indicate that benthic foraminifera may provide evidence for the provenance of coarse sedimentary particles that are deposited into a blue hole, localized hydrodynamics on the flats during hurricane passage may not always promote tempestite deposition in a blue hole (Wallace et al., 2019).

In balance, however, it remains highly likely that at least some sediment with miliolid foraminifers is mobilized, transported

from The Marls, and redeposited into the blue holes during hurricanes. While hydrographic conditions at the sediment-water interface in the blue holes are generally incompatible with foraminiferal ecology (**Figure 8**), we did however observe occasions when the blue hole benthos was at least partially favorable to benthic foraminifera, with slightly higher salinities, more oxygenated conditions, and higher pH. On 29 May 2014, for example, the benthic conditions in both FRSH and MERE were highly oxygenated (>5 mg/L), saline (>27 psu), and alkaline with pH above 7.8 (**Figure 8**). Similarly, the storm event of January 2018 increased dissolved oxygen concentrations in the upper water column in FRSH (**Figure 8**) and the sediment-water interface at ∼5 mbsl was oxic (3.9 mg/L), marine (∼34 psu), and also alkaline (pH 7.6). These conditions likely create more suitable habitat for benthic foraminifera. Based on the homogenous brackish water column measured on 6 January 2018, MERE was most likely discharging meteorically influenced groundwater that filled the entire water column. Given that MAP in the northern Bahamas is less than 1.4 m, the expanded ML observed in FRSH on 6 January 2018 indicates that FRSH was also likely discharging some groundwater from the landscape, but not as much as MERE. In FRSH, coastal groundwater discharge may increase under more intense storm conditions and increased rainfall, prolonging potentially favorable benthic conditions, yet such an event was not observed in this study. It is therefore possible that some passively transported miliolids experience a short-term population bloom following these transiently favorable conditions that may have lasted weeks to months. An alternative hypothesis is that normal tidal exchange of seawater may transport foraminiferal gametes into the blue holes (Whitaker and Smart, 1990; Goldstein, 1997; Alve, 1999; Martin et al., 2012), and in turn these could cause a short-term miliolid population bloom when favorable hydrographic conditions do arise. However, environmental stress caused by a sudden return to benthic dysoxia with dissolved oxygen concentrations <0.3 mg/L, or lowered pH, likely inhibits long-term growth and survival potential of miliolids like *Quinqueloculina, Triloculina* or *Miliolinella* in the blue holes, and contributes to significantly reduced foraminiferal density in the blue holes relative to the adjacent carbonate tidal flats. Either hypothesis, or a combination thereof, would explain why primarily smaller-sized miliolids are observed in the blue holes.

The stressful environmental conditions in MERE and FRSH is further emphasized by a lack of infaunal benthic foraminifera (e.g., *Bolivina*, *Fursenkoina*) in the BHA. Indeed, almost all observed individuals are epifaunal, or near epifaunal, with the exception being the rare occurrence of *Buliminella* in F5 (max 2.3%). Our sites contrast strongly with the benthic foraminifera assemblages found in marine caves of Bermuda, which are flooded by oxygenated marine groundwater (salinity ∼37 psu, pH 8.1, and dissolved oxygen > 3 mg/L), and have large infaunal populations (e.g., *Bolivina* spp. are > 20% of total assemblage) (Cresswell and van Hengstum, 2021). The MERE benthos is persistently anoxic, except potentially during storms when it is likely discharging a mix of saline groundwater and meteoric water (e.g., 6 January 2018 profile with brackish isohaline conditions; **Figure 8**). In contrast, the benthos in FRSH experiences highly variable conditions, which includes recurrent shifts from dysoxic to anoxic conditions during the same calendar year. Infaunal benthic foraminifera are characteristic of assemblages in oxygen depleted environments, which includes oxygen minimum zones (OMZs), fjords, continental sills, and the deep-sea (Bernhard, 1992; Sen Gupta and Machain-Castillo, 1993; Bernhard and Sen Gupta, 1999). Infaunal foraminifera are also common in anoxic deeper-sea areas that experience only brief periods of dysoxia such as the OMZs of California (Bernhard and Bowser, 1999), the Gulf of Mexico (Sen Gupta et al., 1996), and the Arabian Sea (Gooday et al., 2000) where *Quinqueloculina* and *Triloculina* are absent. The lack of infaunal foraminifera in the blue holes suggests that (i) occurrences of any dysoxic to anoxic conditions in the blue holes are too brief to support a substantial infaunal foraminiferal population, (ii) there is very little dissolved oxygen in the porewater below the sediment-water interface, or (iii) other physiochemical conditions in the blue hole prevents infaunal foraminifera from thriving (e.g., low pH, H_2S concentrations).

The most significant faunal differences between the CTFA and the BHA are that the blue holes have (i) increased abundance of the *Ammonia, Cribroelphidium*, *Pseudoeponides*, (ii) typically more agglutinated foraminifera (e.g., *Trochammina*), and (iii) and an increase in the abundance of *Fissurina*. For example, sample BH10 had < 22% of miliolids, with the rest of the assemblage dominated by *Ammonia*, agglutinated foraminifera (e.g., *Trochammina*, *Entzia*), *Pseudoeponides*, and *Cribroelphidium*. Interestingly, *Tiphotrocha* was observed in the stratified subtidal blueholes, and it was also observed in inland stratified sinkholes (cenotes) near the coastline in the Yucatan Peninsula (van Hengstum et al., 2008—misidentified as *Tritaxis fusca*). The disparity in the proportional abundance of *Fissurina* is perhaps related to the suspected ectoparasitic behavior of this taxa (Collen and Newell, 1999), since *Fissurina* is a known ectoparasite of *Rosalina* and *Discorbis* species (Walker et al., 2017). However, *Fissurina* abundances are lowest in the CTFA, where *Rosalina* are common. Alternatively, *Fissurina* has also been observed in various marginal marine environments (Javaux and Scott, 2003; Murray, 2013), with some studies even suggesting tolerance to high total organic carbon and low dissolved oxygen (Bouchet et al., 2018). This ecological possibility is consistent with our observations of higher *Fissurina* abundances within the blue holes. In a meromictic lake on Palau (Jellyfish Lake) that has a comparable stratified water column to the Bahamian blue holes (Hamner et al., 1982), Lipps and Langer (1999) documented that *Ammonia* and *Pseudoeponides* (identified as *Helenina*) dominated shallow water habitats above the chemocline. One could argue that since *Ammonia* and *Cribroelphidium* are present in the shoreline proximal samples (e.g., F1 and F2, **Figure 2**), these taxa are simply transported from these adjacent areas. However, *Pseudoeponides* was only rarely observed in the shoreline proximal samples, yet *Pseudoeponides* appears in higher abundances in the blue holes. Indeed, these taxa are well known from mangrove swamp habitats that produce organic-rich peat deposits in the tropical north Atlantic Ocean (Javaux and Scott, 2003).

However, low productivity in the stunted dwarf red mangroves are not generating widespread peat deposits on the carbonate mudbanks in The Marls of Abaco. While increased geographic coverage of samples on the carbonate tidal flats would increase confidence in the resultant distributions (Verlaak and Collins, 2021), we suggest that the more abundant genera in the BHA (*Ammonia, Cribroelphidium*, *Pseudoeponides*) are most likely part of an *in situ* benthic foraminiferal assemblage in the blue holes.

The ecology of *Ammonia, Cribroelphidium*, *Pseudoeponides* is most compatible with the dynamic hydrographic conditions in the benthos of FRSH and MERE, since these taxa are well known from benthic environments with: (i) low salinity conditions (Brewster-Wingard and Ishman, 1999; Karlsen et al., 2000; van Hengstum et al., 2008), (ii) low dissolved oxygen concentrations (Moodley and Hess, 1992; Sen Gupta and Machain-Castillo, 1993), and low oxygen and pH (Lipps and Langer, 1999). These genera are often considered opportunistic (Hallock et al., 2003), as they can survive in variable conditions like periodic anoxia that are intolerable to most other taxa. In oxygen poor environments, species such as *Ammonia beccarii*, *A. parkinsonia*, and *Cribroelphidium* spp. have been known to survive for days to months (Sen Gupta et al., 1996) potentially due to increased test porosity (Moodley and Hess, 1992), facultative anaerobiosis (Moodley and Hess, 1992), or chloroplast sequestration (Bernhard and Bowser, 1999). *Pseudoeponides* is well-documented for colonizing low salinity habitats globally including inland brackish ponds, sinkholes, and coastal lagoons (Hayward and Hollis, 1994; Javaux and Scott, 2003; Gennari et al., 2011; van Hengstum and Bernhard, 2016), and could tolerate instances of lower salinity in the blueholes. Sen Gupta et al. (1996) specifically used the tolerance of *Ammonia parkinsonia* and *Elphidium* to low oxygen conditions to create an index used to assess prehistoric changes in benthic dissolved oxygen concentrations on the Gulf of Mexico continental shelf. The individual ecology of these taxa suggest that they are most likely transient occupants at the blue hole benthos when hydrographic conditions are favorable.

Hydrographic and Faunal Differences Between the Blue Holes

The Q-mode cluster analysis differentiates the BHA from the CTFA, but subtle foraminiferal differences can also be observed between the samples collected in FRSH vs. MERE. For example, there is a noteworthy difference in the relative abundance of *Ammonia* (FRSH: 4.5%; MERE: 1.7%), *Cribroelphidium* (FRSH: 11.4%; MERE: 2.7%), and *Pseudoeponides* (FRSH: 11.9%; MERE: 2.7%) (**Figure 6**). Additionally, FRSH contains a slightly higher mean abundance of agglutinated foraminifera (*Trochammina*, *Entzia* and *Tiphotrocha*) than MERE (mean agglutinated taxa: FRSH 2.6% vs. MERE 1.5%) (**Figure 5**). These differences are likely tied to the unique hydrography in each blue hole, which includes both (i) the vertical distance between the sediment-water interface and the meteoric lens, and (ii) their inherent hydrogeologic differences. In the bowl-shaped MERE, the depth the sediment-water interface is ∼15 mbsl, with a transition to saline groundwater at 6 m (**Figure 8**). Only after the storm on 6 January 2018 were suitable oxygenated and brackish conditions suitable for brackish-tolerant foraminifera (e.g., *Ammonia*) observed at the MERE sediment-water interface. In contrast, the top of the talus pile in FRSH is ∼5 mbsl, and the zone of meteorically influenced water spans to ∼6 mbsl (**Figure 8**). The upper water column in FRSH is highly dynamic, and frequently becomes oxygenated or slightly brackish during both winters or summers, depending on regional water balance. As such, hydrographic conditions at the sediment-water interface at the top of the talus pile in FRSH is likely more frequently favorable to foraminifera that can tolerate stressful environmental conditions. The vegetation and peat outcrops on the blue hole periphery may be providing further clues to the hydrographic differences between the sites: MERE is the only site with mangrove peat deposits that indicate a more extensive local prehistoric mangrove swamp vs. FRSH, and indeed, the site still supports tree growth (i.e., palms) on a comparatively smaller area of supratidal sediment mound (**Figure 3**). This is consistent with the hydrographic data that suggests that MERE functions as a spring during storm events, which provides the immediate saline-stressed carbonate tidal flats with a source of lower salinity (i.e., meteorically influenced) groundwater. These complex site-specific relationships emphasize the need to constrain modern foraminiferal distributions in blue holes prior to their application as proxies for reconstructing long-term blue hole hydrographic change.

CONCLUSION

This study examines total distributions of benthic foraminifera in two subtidal blue holes in the carbonate tidal flat environment located on the leeward margin of Great Abaco Island, The Bahamas: Freshwater River Blue Hole (FRSH) and Meredith's Blue Hole (MERE). Similar to results from previous work on Bahamian carbonate banktops, marine benthic foraminifera near Abaco form distinct assemblages in leeward vs. windward marine lagoons, carbonate tidal flats, and shoreline proximal areas. Our new results specifically identify new benthic foraminiferal assemblages in the Carbonate Tidal Flats (CTFA), and the subtidal Blue Holes (BHA). Both benthic foraminiferal assemblages are dominated by porcelaneous miliolid taxa like *Triloculina* and *Quinqueloculina*, which exceed 50% in proportional abundance in individual samples. Miliolid taxa commonly occur in well-oxygenated shallow water carbonate systems. However, distinct foraminiferal assemblages in FRSH and MERE were comprised of small-sized miliolids and statistically significant proportions of taxa that are known to tolerate both brackish, oxygen-depleted, and organic-rich conditions (e.g., *Ammonia*, *Cribroelphidium*, etc.). It is possible that these taxa experience short-term population blooms in response to favorable conditions at the sediment-water interface driven by hydroclimate changes or storm activity. Hydrographically, the two blue holes examined were slightly different: MERE remained more persistently stratified through

different seasons, but the blue hole discharged a large volume of meteorically influenced water after a storm event on 8 January 2018 (i.e., spring). In contrast, stratification in FRSH was highly variable and groundwater springing was not as environmentally dominant as in FRSH. The most notable faunal differences between the CTFA and BHA occurred in the secondary or non-miliolid taxa, and they indicate that a unique benthic environment exists in the subtidal blue holes. The secondary taxa with >5% in the CTFA includes taxa commonly found throughout the Caribbean and previously observed platform interior of the Little Bahama Bank (i.e., *Rotorbis*, *Archaias*, and *Rosalina*), while the BHA contains a greater proportion of stress-tolerant taxa including *Pseudoeponides*, *Cribroelphidium,* and *Ammonia*. Furthermore, the BHA is the only assemblage to contain agglutinated taxa like *Trochammina*, *Entzia*, and *Tiphotrocha*.

DATA AVAILABILITY STATEMENT

The original contributions presented in the study are included in the article/**Supplementary Material**, further inquiries can be directed to the corresponding author/s.

AUTHOR CONTRIBUTIONS

PvH, JD, NA, and SL contributed to the conception and design of the study. PvH, JD, and NA provided essential resources for data collection and analysis. SL organized the database, analyzed and interpreted the results, created all the figures and tables, and wrote the first draft of the manuscript. PvH, PB, JD, TW, and SL contributed to sections of the manuscript and edits to the figures and tables. All authors contributed to the various aspects of sample collection and field observations, and reviewed and approved the final version of the manuscript for submission.

FUNDING

The financial support for this work was provided by grants from the National Science Foundation to PvH (EAR-1833117) and JD (EAR-1702946).

ACKNOWLEDGMENTS

The field support was provided by Friends of the Environment, Michael Albury, Captain Jody Albury, Victoria Keeton, Richard Sullivan, Anne Tamalavage, Elizabeth Wallace, and Brian Kakuk. The authors have also benefited from discussions on Bahamian hydrogeology with Jason Gulley and Alex Mayer. Sediment samples were collected and exported for analysis with the support of The Bahamas Environment, Science, and Technology Commission through scientific permits issued to PvH and JD in 2014 and 2016. No work on DNA or live specimens or animals occurred during the course of this work.

SUPPLEMENTARY MATERIAL

The Supplementary Material for this article can be found online at: https://www.frontiersin.org/articles/10.3389/fevo.2021.794728/full#supplementary-material

REFERENCES

Allen, G. M., and Barbour, T. (1904). Narrative of a Trip to the Bahamas. *Linn. Fem Bull.* 4, 11–12. doi: 10.5962/bhl.title.48678

Alve, E. (1999). Colonization of new habitats by benthic foraminifera: a review. *Earth Sci. Rev.* 46, 167–185. doi: 10.1016/S0012-8252(99)00016-1

Beddows, P. A., and Mallon, E. K. (2018). Cave pearl data logger: a flexible Arduino-based logging platform for long-term monitoring in harsh environments. *Sensors* 18:530. doi: 10.3390/s18020530

Beddows, P. A., Smart, P. L., Whitaker, F. F., and Smith, S. L. (2007). Decoupled fresh-saline groundwater circulation of a coastal carbonate aquifer: spatial patterns of temperature and specific electrical conductivity. *J. Hydrol.* 346, 18–32. doi: 10.1016/j.jhydrol.2007.08.013

Bergamin, L., Ruggerio, E. T., Pierfrancheschi, G., Andres, B., Costantino, R., Crovato, C., et al. (2020). Benthic foraminifera and brachiopods from a marine cave in Spain: environmental significance. *Mediterr. Mar. Sci.* 21, 506–518. doi: 10.12681/mms.23482

Bernhard, J. M. (1992). Benthic foraminiferal distribution and biomass related to pore-water oxygen content: central California continental slope and rise. *Deep Sea Res. A. Oceanogr. Res. Pap.* 39, 585–605. doi: 10.1016/0198-0149(92)90090-G

Bernhard, J. M., and Bowser, S. S. (1999). Benthic foraminifera of dysoxic sediments: chloroplast sequestration and functional morphology. *Earth Sci. Rev.* 46, 149–165. doi: 10.1016/S0012-8252(99)00017-3

Bernhard, J. M., and Sen Gupta, B. K. (1999). "Foraminifera of oxygen-depleted environments," in *Modern Foraminifera*, ed. B. K. Sen Gupta (Dordrecht: Springer), 201–216. doi: 10.1007/0-306-48104-9_12

Bethke, C., Lee, M., and Park, J. (2007). *Basin Modeling with Basin 2, a Guide to Using the Basin2 Software Package, Release 5.0. 1. Hydrogeology Program*. Champaign: University of Illinois.

Bock, W. D. (1971). "A Handbook of the Benthonic Foraminifera of Florida Bay and Adjacent Waters," in *A Symposium of Recent South Florida Foraminifera*, eds J. I. Jones and W. D. Bock (Florida: Miami Geological Society).

Bouchet, V. M., Telford, R. J., Rygg, B., Oug, E., and Alve, E. (2018). Can benthic foraminifera serve as proxies for changes in benthic macrofaunal community structure? Implications for the definition of reference conditions. *Mar. Environ. Res.* 137, 24–36. doi: 10.1016/j.marenvres.2018.02.023

Brady, H. B. (1870). The Ostracoda and Foraminifera of tidal rivers. With an analysis and descriptions of the Foraminifera, by Henry B. Brady, F.L.S. *Ann. Mag. Nat. Hist.* 6, 273–309.

Brady, H. B. (1884). Report on the foraminifera dredged by H.M.S Challenger during the years 1873-1876. *Zoology* 9, 1–115.

Brewster-Wingard, G. L., and Ishman, S. E. (1999). Historical trends in salinity and substrate in central Florida Bay: a paleoecological reconstruction using modern analogue data. *Estuaries* 22, 369–383. doi: 10.2307/1353205

Buzas, M. A. (1968). On the spatial distribution of foraminifera. *J. Foraminifer. Res.* 19, 1–11.

Cant, R. V., and Weech, P. S. (1986). A review of the factors affecting the development of Ghyben-Hertzberg lenses in the Bahamas. *J. Hydrol.* 84, 333–343. doi: 10.1016/0022-1694(86)90131-9

Carmen, K. W. (1927). *The shallow-water foraminifera of Bermuda*. (Ph.D. thesis). Cambridge: Massachusetts Institute of Technology.

Charrieau, L. M., Filipsson, H. L., Ljung, K., Chierici, M., Knudsen, K. L., and Kritzberg, E. (2018). The effects of multiple stressors on the distribution of

coastal benthic foraminifera: a case study from the Skagerrak-Baltic Sea region. *Mar. Micropaleontol.* 139, 42–56. doi: 10.1016/j.marmicro.2017.11.004

Cheng, J., Collins, L. S., and Holmes, C. (2012). Four thousand years of habitat change in Florida Bay, as indicated by Benthic Foraminifera. *J. Foraminifer. Res.* 42, 3–17. doi: 10.2113/gsjfr.42.1.3

Clarke, K. R. (1993). Non-parametric multivariate analyses of changes in community structure. *Aust. J. Ecol.* 18, 117–143. doi: 10.1111/j.1442-9993.1993.tb00438.x

Cole, L. G. (1910). The caverns and people of the northern Yucatan. *Bull. Am. Geogr. Soc.* 42, 321–336. doi: 10.2307/199038

Cole, W. S. (1931). The Pliocene and Pleistocene Foraminifera of Florida. *Florida Geol. Surv. Bull.* 6, 182–190.

Collen, J. D., and Newell, P. (1999). Fissurina as an ectoparasite. *J. Micropalaeontol.* 18, 110–110. doi: 10.1144/jm.18.2.110

Colwell, R. K., Chao, A., Gotelli, N. J., Lin, S.-Y., Mao, C. X., Chazdon, R. L., et al. (2012). Models and estimators linking individual-based and sample-based rarefaction, extrapolation and comparison of assemblages. *J. Plant Ecol.* 5, 3–21. doi: 10.1093/jpe/rtr044

Cresswell, J. N., and van Hengstum, P. J. (2021). Habitat Partitioning in the Marine Sector of Karst Subterranean Estuaries and Bermuda's Marine Caves: benthic Foraminiferal Evidence. *Front. Environ. Sci.* 8:594554. doi: 10.3389/fenvs.2020.594554

Culver, S. J., and Buzas, M. A. (1982). *Distribution Of Recent Benthic Foraminifera In The Caribbean Region*. Washington: Smithsonian Institution Press. doi: 10.5479/si.01960768.14.1

Cushman, J. A. and Brönnimann, P. (1948). Additional new species of arenaceous foraminifera from shallow water of Trinidad. *Contr. Lab. Foraminifer. Res.* 24, 37–42. doi: 10.4159/harvard.9780674330863.c6

d'Orbigny, A. (1826). Tableau méthodique de la classe des Céphalopodes. *Ann. Sci. Nat.* 7, 96–169.

d'Orbigny, A. (1839a). "Foraminifères," in *Histoire physique, politique et naturelle de l'ile de Cuba*, ed. R. de la Sagra (Paris: A. Bertrand).

d'Orbigny, A. (1839b). *Voyage dans l'Amérique Méridionale-Foraminifères*. Strasbourg: Levrault.

Fall, P. L., van Hengstum, P. J., Lavold-Foote, L., Donnelly, J. P., Albury, N. A., and Tamalavage, A. E. (2021). Human arrival and landscape dynamics in the northern Bahamas. *Proc. Natl. Acad. Sci. U. S. A.* 118:e2015764118. doi: 10.1073/pnas.2015764118

Fatela, F., and Taborda, R. (2002). Confidence limits of species proportions in microfossil assemblages. *Mar. Micropaleontol.* 45, 169–174. doi: 10.1016/S0377-8398(02)00021-X

Fichtel, L. V., and Moll, J. P. C. (1798). *Testacea microscopia*, aliaque minuta ex generibus Argonauta et nautilus, ad naturam delineata et descripta. *Pichler Wien* 123.

Fischel, A., Seidenkrantz, M.-S., and Vad Odgaard, B. (2018). Benthic foraminiferal assemblages and test accumulation in coastal microhabitats on San Salvador, Bahamas. *J. Micropalaeontol.* 37, 499–518. doi: 10.5194/jm-37-499-2018

Forskål, P. (1775). *Descriptiones animalium, avium, amphibiorum, piscium, insectorum, vermium: quae in itinere orientali observavit*. Copengagen: ex officina Mölleri. doi: 10.5962/bhl.title.2154

Gennari, G., Rosenberg, T., Spezzaferri, S., Berger, J.-P., Fleitmann, D., Preusser, F., et al. (2011). Faunal evidence of a Holocene pluvial phase in southern Arabia with remarks on the morphological variability of Helenina anderseni. *J. Foraminifer. Res.* 41, 248–259.

Goldstein, S. T. (1997). Gametogenesis and the antiquity of reproductive pattern in the foraminiferida. *J. Foraminifer. Res.* 27, 319–328. doi: 10.2113/gsjfr.27.4.319

Gooday, A. J., Bernhard, J. M., Levin, L. A., and Suhr, S. B. (2000). Foraminifera in the Arabian Sea oxygen minimum zone and other oxygen-deficient settings: taxonomic composition, diversity, and relation to metazoan faunas. *Deep Sea Res. II Top. Stud. Oceanogr.* 47, 25–54. doi: 10.1016/S0967-0645(99)00099-5

Gotelli, N. J., and Colwell, R. K. (2011). "Estimating species richness," in *Biological Diversity: Frontiers in Measurement and Assessment*, eds A. E. Magurran and B. J. McGill (Oxford: Oxford University Press), 39–54.

Gulley, J. D., Mayer, A. S., Martin, J. B., and Bedekar, V. (2016). Sea level rise and inundation of island interiors: assessing impacts of lake formation and evaporation on water resources in arid climates. *Geophys. Res. Lett.* 43, 9712–9719. doi: 10.1002/2016GL070667

Haas, S., de Beer, D., Klatt, J. M., Fink, A. H., Rench, R. M., Hamilton, T. L., et al. (2018). Low-Light Anoxygenic Photosynthesis and Fe-S-Biogeochemistry in a Microbial Mat. *Front. Microbiol.* 9:858. doi: 10.3389/fmicb.2018.00858

Hallock, P., Lidz, B. H., Cockey-Burkhard, E. M., and Donnelly, K. B. (2003). Foraminifera as bioindicators in coral reef assessment and monitoring: the FORAM index. *Environ. Monit. Assess.* 81, 221–238. doi: 10.1023/A:1021337310386

Hamner, W. M., Gilmer, R. W., and Hamner, P. P. (1982). The physical, chemical, and biological characteristics of a stratified, saline, sulfide lake in Palau. *Limnol. Oceanogr.* 27, 896–909. doi: 10.4319/lo.1982.27.5.0896

Hawkes, A. D., Bird, M., Cowie, S., Grundy-Warr, C., Horton, B. P., Shau Hwia, A. T., et al. (2007). Sediments deposited by the 2004 Indian Ocean Tsunamic along the Malaysia-Thailand Peninsula. *Mar. Geol.* 242, 169–190.

Hayward, B. W., and Hollis, C. J. (1994). Brackish foraminifera in New Zealand; a taxonomic and ecologic review. *Micropaleontology* 40, 185–222. doi: 10.2307/1485816

Hodell, D. A., Brenner, M., and Curtis, J. H. (2005). Terminal Classic drought in the northern Maya lowlands inferred from multiple sediment cores in Lake Chichancanab (Mexico). *Quat. Sci. Rev.* 24, 1413–1427. doi: 10.1016/j.quascirev.2004.10.013

Javaux, E. J., and Scott, D. B. (2003). Illustration of modern benthic foraminifera from Bermuda and remarks on distribution in other subtropical/tropical areas. *Palaeontol. Electronica* 6:29.

Jury, M., Malmgren, B. A., and Winter, A. (2007). Subregional precipitation climate of the Caribbean and relationships with ENSO and NAO. *J. Geophys. Res. Atmos.* 112:D16107. doi: 10.1029/2006JD007541

Kaiho, K. (1994). Benthic foraminiferal dissolved-oxygen index and dissolved-oxygen levels in the modern ocean. *Geology* 22, 719–722.

Kaiho, K. (1999). Effect of organic carbon flux and dissolved oxygen on the benthic foraminiferal oxygen index (BFOI). *Mar. Micropaleontol.* 37, 67–76. doi: 10.1016/S0377-8398(99)00008-0

Karlsen, A. W., Cronin, T. M., Ishman, S. E., Willard, D. A., Kerhin, R., Holmes, C. W., et al. (2000). Historical trends in Chesapeake Bay dissolved oxygen based on benthic foraminifera from sediment cores. *Estuaries* 23, 488–508. doi: 10.2307/1353141

Kjellmark, E. (1996). Late Holocene climate change and human disturbance on Andros Island, Bahamas. *J. Paleolimnol.* 15, 133–145. doi: 10.1007/BF00196777

Koch, M. S., and Snedaker, S. C. (1997). Factors influencing *Rhizophora mangle* L. seedling development in Everglades carbonate soils. *Aquat. Bot.* 59, 87–98.

Lane, P., Donnelly, J. P., Woodruff, J. D., and Hawkes, A. D. (2011). A decadally-resolved paleohurricane record archived in the late Holocene sediments of a Florida sinkhole. *Mar. Geol.* 287, 14–30. doi: 10.1016/j.margeo.2011.07.001

Legendre, P., and Legendre, L. (1998). *Numerical Ecology: second English edition*. Amsterdam: Elsevier.

Li, C., and Jones, B. (1997). Comparison of foraminiferal assemblages in sediments on the windward and leeward shelves of Grand Cayman, British West Indies. *Palaios* 12, 12–26. doi: 10.2307/3515291

Lidz, B. H., and Rose, P. R. (1989). Diagnostic foraminiferal assemblages of Florida Bay and adjacent shallow waters: a comparison. *Bull. Mar. Sci.* 44, 399–418.

Lin, G., and Sternberg, L. D. S. (1992). Effect of growth form, salinity, nutrient and sulfide on photosynthesis, carbon isotope discrimination and growth of red mangrove (*Rhizophora mangle* L.). *Funct. Plant Biol.* 19, 509–517. doi: 10.1071/PP9920509

Linnaeus, C. (1758). *Systema naturae per regna tria naturae, secundum classes, ordines, genera, species, cum characteribus, differentiis, synonymis, locis*. Holmiae: Laurentius Salvius. doi: 10.5962/bhl.title.542

Lipps, J. H., and Langer, M. R. (1999). Benthic Foraminifera from the Meromictic Mecherchar Jellyfish Lake, Palau (Western Pacific). *Micropaleontology* 45, 278–284. doi: 10.2307/1486137

Little, S. N., and van Hengstum, P. J. (2019). Intertidal and subtidal benthic foraminifera in flooded caves: implications for reconstructing coastal karst aquifers and cave paleoenvironments. *Mar. Micropaleontol.* 149, 19–34. doi: 10.1016/j.marmicro.2019.03.005

Macario-González, L., Cohuo, S., Angyal, D., Pérez, L., and Mascaró, M. (2021). Subterranean Waters of Yucatán Peninsula, Mexico Reveal Epigean Species Dominance and Intraspecific Variability in Freshwater Ostracodes (Crustacea: Ostracoda). *Diversity* 13:44. doi: 10.3390/d13020044

Maloof, A. C., and Grotzinger, J. P. (2012). The Holocene shallowing-upward parasequence of north-west Andros Island, Bahamas. *Sedimentology* 59, 1375–1407. doi: 10.1111/j.1365-3091.2011.01313.x

Martin, J. B., Gulley, J., and Spellman, P. (2012). Tidal pumping of water between Bahamian blue holes, aquifers, and the ocean. *J. Hydrol.* 416, 28–38. doi: 10.1016/j.jhydrol.2011.11.033

Montagu, G. (1803). *Testacea Britannica, or Natural History of British Shells, Marine, Land, and Fresh-Water, Including the Most Minute*. Romsey: Hollis.

Moodley, L., and Hess, C. (1992). Tolerance of infaunal benthic foraminifera for low and high oxygen concentrations. *Biol. Bull.* 183, 94–98. doi: 10.2307/1542410

Murray, J. W. (2000). The enigma of the continued use of total assemblage in ecological studies of benthic foraminifera. *J. Foraminifer. Res.* 30, 244–245. doi: 10.2113/0300244

Murray, J. W. (2013). Living benthic foraminifera: biogeographical distributions and the significance of rare morphospecies. *J. Micropalaeontol.* 32, 1–58.

Mylroie, J. E., Carew, J. L., and Moore, A. I. (1995). Blue holes: definition and genesis. *Carbonates Evaporites* 10, 225–233. doi: 10.1007/BF03175407

Neumann, A. C., and Land, L. S. (1975). Lime mud deposition and calcareous algae in the Bight of Abaco, Bahamas: a budget. *J. Sed. Res.* 45, 763–786. doi: 10.1306/212F6E3D-2B24-11D7-8648000102C1865D

Parker, F. L. (1962). Quinqueloculina tenagos, new name for Quinqueloculina rhodiensis Parker, preoccupied. *Contrib. Cushman Found. Foraminifer. Res.* 13:110.

Patin, N., Dietrich, Z., Stancil, A., Quinan, M., Beckler, J., Hall, E., et al. (2020). Gulf of Mexico blue hole harbors high levels of novel microbial lineages. *bioRxiv* [Preprint]. doi: 10.1101/2020.10.18.342550

Patterson, R. T., and Fishbein, E. (1989). Re-examination of the statistical methods used to determine the number of point counts needed for micropaleontological quantitative research. *J. Paleontol.* 63, 245–248. doi: 10.1017/S0022336000019272

Peros, M., Collins, S., Agosta G'Meiner, A., Reinhardt, E., and Pupo, F. M. (2017). Multistage 8.2 kyr event revealed through high-resolution XRF core scanning of Cuban sinkhole sediments. *Geophys. Res. Lett.* 44, 7374–7381. doi: 10.1002/2017GL074369

Pilarczyk, J. E., Reinhardt, E. G., Boyce, J. I., Schwarcz, H. P., and Donato, S. V. (2011). Assessing surficial foraminiferal distributions as an overwash indicator in Sur Lagoon, Sultanate of Oman. *Mar. Micropaleonol.* 80, 62–73. doi: 10.1016/j.marmicro.2011.06.001

Pilskaln, C. H., Neumann, A. C., and Bane, J. M. (1989). Periplatform carbonate flux in the northern Bahamas. *Deep Sea Res. A. Oceanogr. Res. Pap.* 36, 1391–1406. doi: 10.1016/0198-0149(89)90090-3

R Core Team (2021). *R: A language and environment for statistical computing*. Vienna: R Project for Statistical Computing. Retrieved from https://www.R-project.org/

Rasmussen, K. A., Haddad, R. I., and Neumann, A. C. (1990). Stable-isotope record of organic carbon from an evolving carbonate banktop, Bight of Abaco, Bahamas. *Geology* 18, 790–794. doi: 10.1130/0091-7613(1990)018<0790:SIROOC>2.3.CO;2

Romano, E., Bergamin, L., Di Bella, L., Frezza, V., Marassich, A., Pierfranceschi, G., et al. (2020). Benthic foraminifera as proxies of marine influence in the Orosei marine caves (Sardinia, Italy). *Aquat. Conserv.* 30, 701–716. doi: 10.1002/aqc.328

Romano, E., Bergamin, L., Pierfranceschi, G., Provenzani, C., and Marassich, A. (2018). The distribution of benthic foraminifera in Bel Torrente submarine cave (Sardinia, Italy) and their environmental significance. *Mar. Environ. Res.* 133, 114–127. doi: 10.1016/j.marenvres.2017.12.014

Rose, P. R., and Lidz, B. H. (1977). *Diagnostic foraminiferal assemblages of shallow-water modern environments : South Florida and the Bahamas (Sedimenta, vol V])*. Florida: University of Miami.

Rossi, R. E., Archer, S. K., Giri, C., Layman, C. A. (2020). The role of multiple stressors in a dwarf red mangrove (*Rhizophora mangle*) dieback. *Estuar. Coast. Shelf Sci.* 237:106660. doi: 10.1016/j.ecss.2020.106660

Saraswat, R., Nigam, R., and Pachkhande, S. (2011). Difference in optimum temperature for growth and reproduction in benthic foraminifer Rosalina globularis: implications for paleoclimatic studies. *J. Exp. Mar. Biol. Ecol.* 405, 105–110.

Scott, D. B., and Hermelin, J. (1993). A device for precision splitting of micropaleontological samples in liquid suspension. *J. Paleontol.* 67, 151–154. doi: 10.1017/S0022336000021302

Scott, D. B., and Medioli, F. S. (1980). Living vs. total foraminiferal populations: their relative usefulness in paleoecology. *J. Paleontol.* 54, 814–813.

Sellier de Civrieux, J. M. (1977). *Las Discorbidae de Mar Caribe, frente a Venezuela*. Venezuela: Universidad de Oriente, 1–46.

Sen Gupta, B. K., Eugene Turner, R., and Rabalais, N. N. (1996). Seasonal oxygen depletion in continental-shelf waters of Louisiana: historical record of benthic foraminifers. *Geology* 24, 227–230. doi: 10.1130/0091-7613(1996)024<0227:SODICS>2.3.CO;2

Sen Gupta, B. K., and Machain-Castillo, M. L. (1993). Benthic foraminifera in oxygen-poor habitats. *Mar. Micropaleontol.* 20, 183–201. doi: 10.1016/0377-8398(93)90032-S

Shinn, E. A., Lloyd, R. M., and Ginsburg, R. N. (1969). Anatomy of a modern carbonate tidal-flat, Andros Island, Bahamas. *J. Sed. Res.* 39, 1202–1228. doi: 10.1306/74D71DCF-2B21-11D7-8648000102C1865D

Shinn, E. A., Reich, C. D., Locker, S. D., and Hine, A. C. (1996). A giant sediment trap in the Florida Keys. *J. Coast. Res.* 12, 953–959.

Smart, C. C. (1984). The hydrology of the inland blue holes, Andros Island. *Cave Sci.* 11, 23–29.

Smart, P. L., Dawans, J. M., and Whitaker, F. (1988). Carbonate dissolution in a modern mixing zone. *Nature* 355, 811–813. doi: 10.1038/335811a0

Socki, R. A., Perry, E. C., and Romanek, C. S. (2002). Stable isotope systematics of two cenotes from the northern Yucatan Peninsula, Mexico. *Limnol. Oceanogr.* 47, 1808–1818. doi: 10.4319/lo.2002.47.6.1808

Steadman, D. W., Franz, R., Morgan, G. S., Albury, N. A., Kakuk, B., Broad, K., et al. (2007). Exceptionally well preserved late Quaternary plant and vertebrate fossils from a blue hole on Abaco, The Bahamas. *Proc. Natl. Acad. Sci. U. S. A.* 104, 19897–19902.

Sullivan, R. M., van Hengstum, P. J., Donnelly, J. P., Winkler, T. S., Mark, S. E., and Albury, N. A. (2020). Absolute and relative dating of human remains in a Bahamian sinkhole (Great Cistern, Abaco). *J. Archaeol. Sci. Rep.* 32:102441. doi: 10.1016/j.jasrep.2020.102441

Teeter, J. W. (1995). "). Holocene saline lake history, San Salvador Island, Bahamas," in *Terrestrial and Shallow Marine Geology of the Bahamas and Bermuda*, eds H. A. Curan and B. White (Colorado: Geological Society of America), 117–124. doi: 10.1130/0-8137-2300-0.117

Todd, R., and Low, D. (1971). Foraminifera from the Bahama Bank West of Andros Island. *U. S. Geol. Surv. Profess. Pap.* 683-C, 1–22.

Uthicke, S., Momigliano, P., and Fabricius, K. E. (2013). High risk of extinction of benthic foraminifera in this century due to ocean acidification. *Sci. Rep.* 3:1769. doi: 10.1038/srep01769

van Hengstum, P. J., and Bernhard, J. M. (2016). A new species of benthic foraminifera from an inland Bahamian carbonate marsh. *J. Foraminifer. Res.* 46, 193–200. doi: 10.2113/gsjfr.46.2.193

van Hengstum, P. J., Donnelly, J. P., Fall, P. L., Toomey, M. R., Albury, N. A., and Kakuk, B. (2016). The intertropical convergence zone modulates intense hurricane strikes on the western North Atlantic margin. *Sci. Rep.* 6:21728. doi: 10.1038/srep21728

van Hengstum, P. J., Maale, G., Donnelly, J. P., Albury, N. A., Onac, B. P., Sullivan, R. M., et al. (2018). Drought in the northern Bahamas from 3300 to 2500 years ago. *Quat. Sci. Rev.* 186, 169–185. doi: 10.1016/j.quascirev.2018.02.014

van Hengstum, P. J., Reinhardt, E. G., Beddows, P. A., and Gabriel, J. J. (2010). Investigating linkages between Holocene paleoclimate and paleohydrogeology preserved in a Yucatan underwater cave. *Quat. Sci. Rev.* 29, 2788–2798. doi: 10.1016/j.quascirev.2010.06.034

van Hengstum, P. J., Reinhardt, E. G., Beddows, P. A., Huang, R. J., and Gabriel, J. J. (2008). Thecamoebians (testate amoebae) and foraminifera from three anchialine cenotes in Mexico: low salinity (1.5–4.5 psu) faunal transitions. *J. Foraminifer. Res.* 38, 305–317. doi: 10.2113/gsjfr.38.4.305

van Hengstum, P. J., and Scott, D. B. (2011). Ecology of foraminifera and habitat variability in an underwater cave: distinguishing anchialine versus submarine cave environments. *J. Foraminifer. Res.* 41, 201–229.

van Hengstum, P. J., Scott, D. B., Gröcke, D. R., and Charette, M. A. (2011). Sea level controls sedimentation and environments in coastal

caves and sinkholes. *Mar. Geol.* 286, 35–50. doi: 10.1016/j.margeo.2011.05.004

van Hengstum, P. J., Winkler, T. S., Tamalavage, A. E., Sullivan, R. M., Little, S. N., Donnelly, J. P., et al. (2020). Holocene sedimentation in a blue hole surrounded by carbonate tidal flats in The Bahamas: autogenic versus allogenic processes. *Mar. Geol.* 419:106051.

Verlaak, Z. R., and Collins, L. S. (2021). Environmental Controls on the Distribution of Modern Benthic Foraminifera in the Florida Everglades and Their Use as Paleoenvironmental Indicators. *J. Foraminifer. Res.* 51, 182–209. doi: 10.2113/gsjfr.51.3.182

Walker, S. E., Hancock, L. G., and Bowser, S. S. (2017). Diversity, biogeography, body size and fossil record of parasitic and suspected parasitic foraminifera: a review. *J. Foraminifer. Res.* 47, 34–55. doi: 10.2113/gsjfr.47.1.34

Wallace, E., Donnelly, J., van Hengstum, P., Wiman, C., Sullivan, R., Winkler, T., et al. (2019). Intense hurricane activity over the past 1500 years at South Andros Island, The Bahamas. *Paleoceanogr. Paleoclimatol.* 34, 1761–1783.

Wang, Y., Van Beynen, P., Wang, P., Brooks, G., Herbert, G., and Tykot, R. (2021). Investigation of sedimentary records of Hurricane Irma in sinkholes, Big Pine Key, Florida. *Prog. Phys. Geogr. Earth Environ.* 18, 1–22. doi: 10.1177/03091333211017764

Warren, A. (1957). Foraminifera of the Buras-Scofield bayou region, southeast Louisiana. *Contrib. Cushman Found. Foraminifer. Res.* 8, 29–40.

Warton, D. I., Wright, S. T., and Wang, Y. (2012). Distance-based multivariate analyses confound location and dispersion effects. *Methods Ecol. Evol.* 3, 89–101. doi: 10.1111/j.2041-210X.2011.00127.x

Whitaker, F., and Smart, P. (1990). Active circulation of saline ground waters in carbonate platforms: evidence from the Great Bahama Bank. *Geology* 18, 200–203. doi: 10.1130/0091-7613(1990)018<0200:ACOSGW>2.3.CO;2

Whitaker, F. F., and Smart, P. L. (1997). "Hydrogeology of the Bahamian archipelago," in *Geology and Hydrogeology of Carbonate Islands*, eds H. L. Vacher and T. M. Quinn (Amsterdam: Elsevier), 183–216. doi: 10.1016/S0070-4571(04)80026-8

Wilson, B. (2006). The environmental significance of *Archaias angulatus* (miliolida, foraminifera) in sediments around Nevis, West Indies. *Caribb. J. Sci.* 42, 20–23.

Winkler, T. S., van Hengstum, P. J., Donnelly, J. P., Wallace, E. J., Sullivan, R. M., MacDonald, D., et al. (2020). Revising evidence of hurricane strikes on Abaco Island (The Bahamas) over the last 700 years. *Sci. Rep.* 10:16556. doi: 10.1038/s41598-020-73132-x

WoRMS Editorial Board (2021). *World Register of Marine Species*. doi: 10.14284/170 Available online at: http://www.marinespecies.org.

Zarikian, C. A. A., Swart, P. K., Gifford, J. A., and Blackwelder, P. L. (2005). Holocene paleohydrology of Little Salt Spring, Florida, based on ostracod assemblages and stable isotopes. *Palaeogeogr. Palaeoclimatol. Palaeoecol.* 225, 134–156. doi: 10.1016/j.palaeo.2004.01.023

Conflict of Interest: The authors declare that the research was conducted in the absence of any commercial or financial relationships that could be construed as a potential conflict of interest.

Publisher's Note: All claims expressed in this article are solely those of the authors and do not necessarily represent those of their affiliated organizations, or those of the publisher, the editors and the reviewers. Any product that may be evaluated in this article, or claim that may be made by its manufacturer, is not guaranteed or endorsed by the publisher.